

Supplementary Appendix 1: Figures

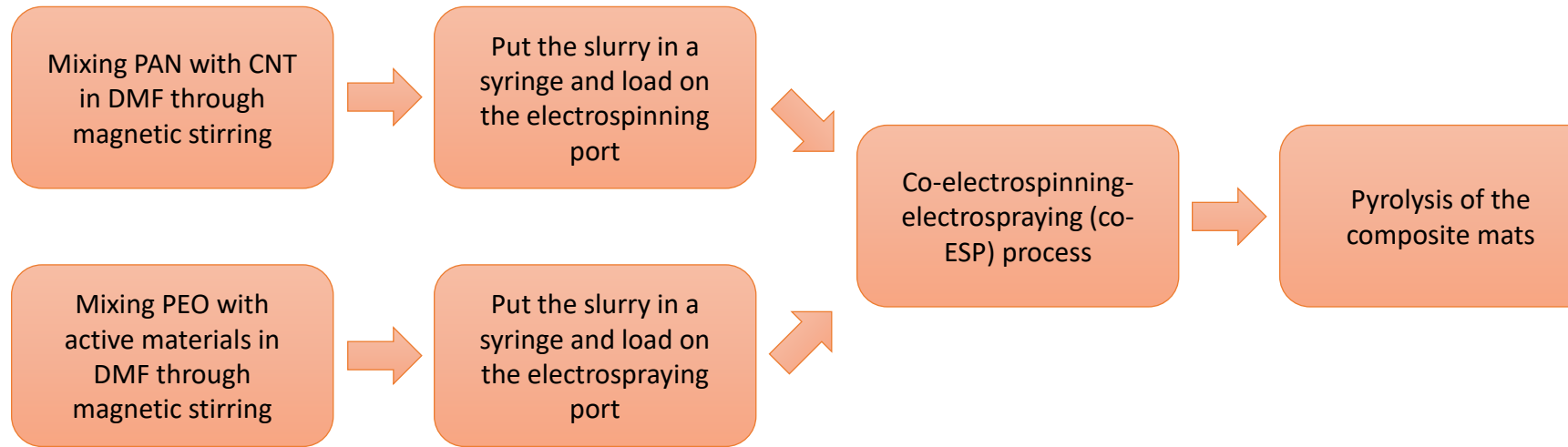


Figure S1 Flow chart showing the process of fabricating co-ESP electrode

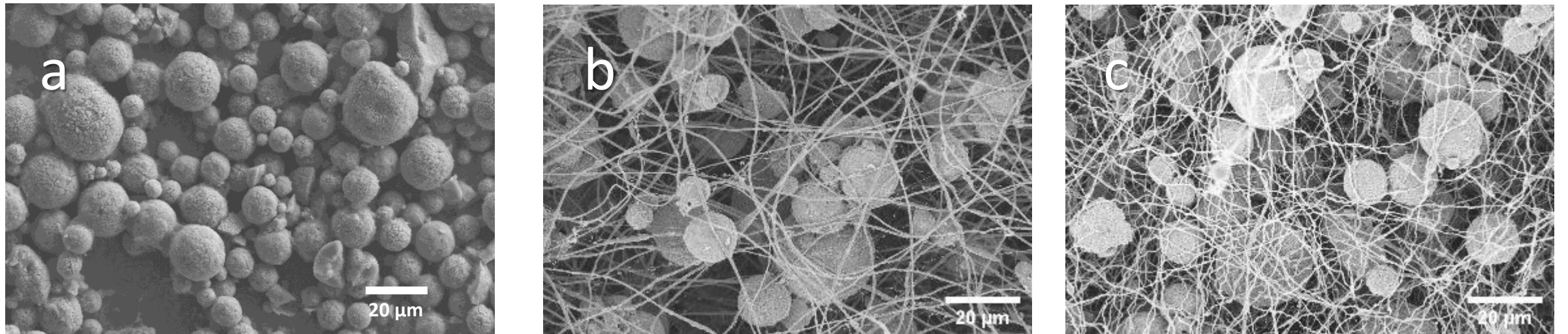


Figure S2 Morphology of a. Pristine NVPC particles; b. NVPC-PEO/PAN-CNT composite mat, right after the co-ESP fabrication; c. NVPC/CNT-CNF electrode, after pyrolysis.

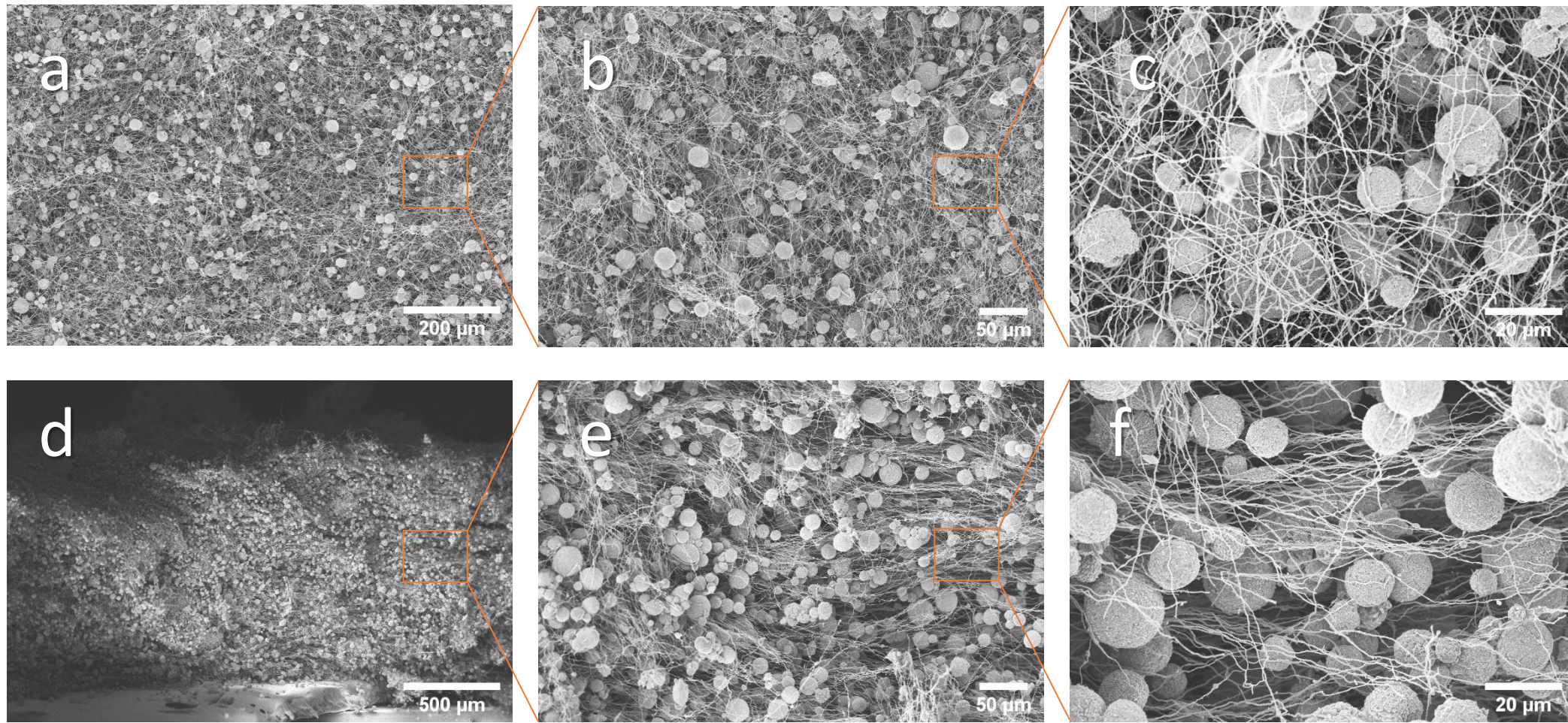


Figure S3 Morphology of 97.5% NVPC/CNTF from **a-c.** top view and **d-f.** cross view of different magnifications

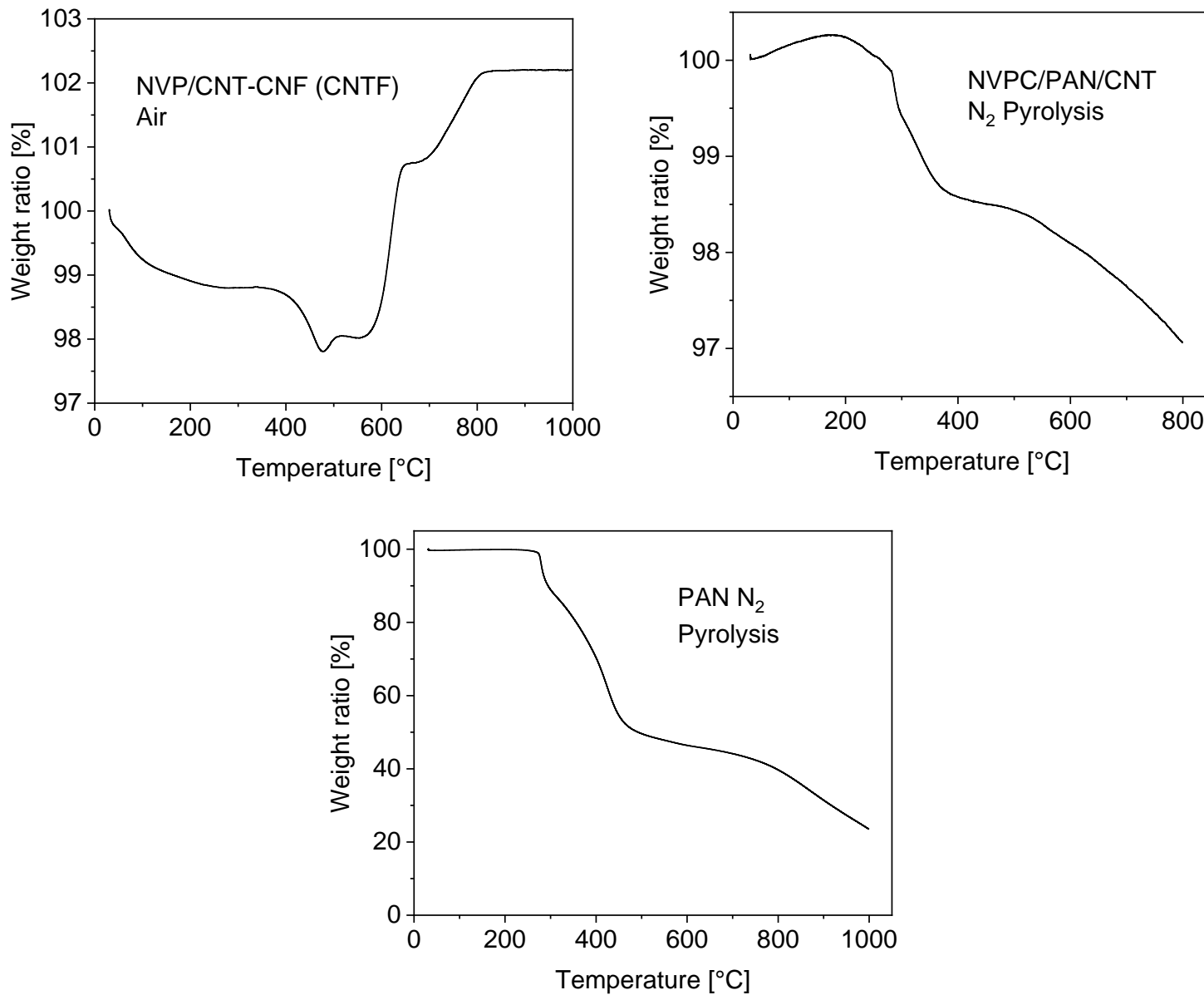


Figure S4 TGA of NVPC/CNTF in air, NVPC/PAN-CNT right after co-ESP fabrication in N₂ and pure PAN fibres in N₂

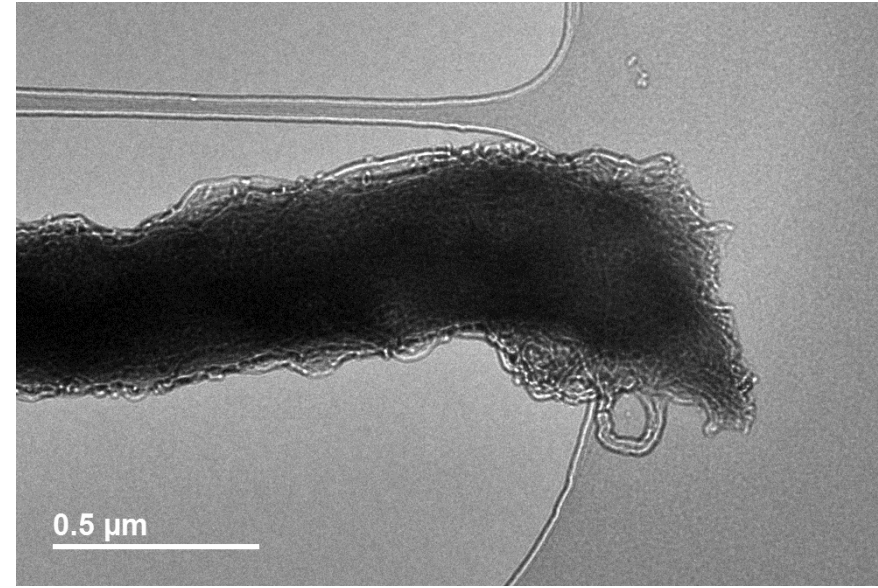
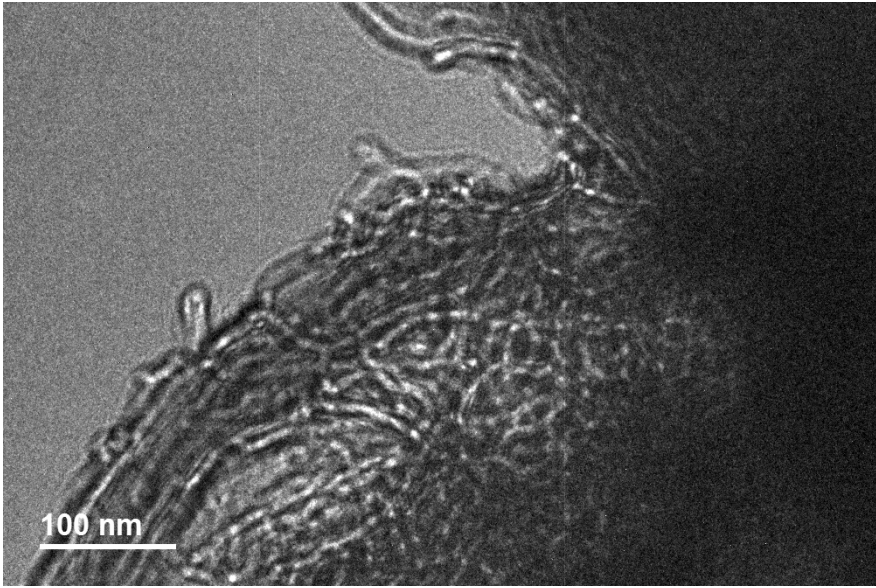


Figure S5 TEM of carbon nanotube embedded carbon fibre (CNTF)

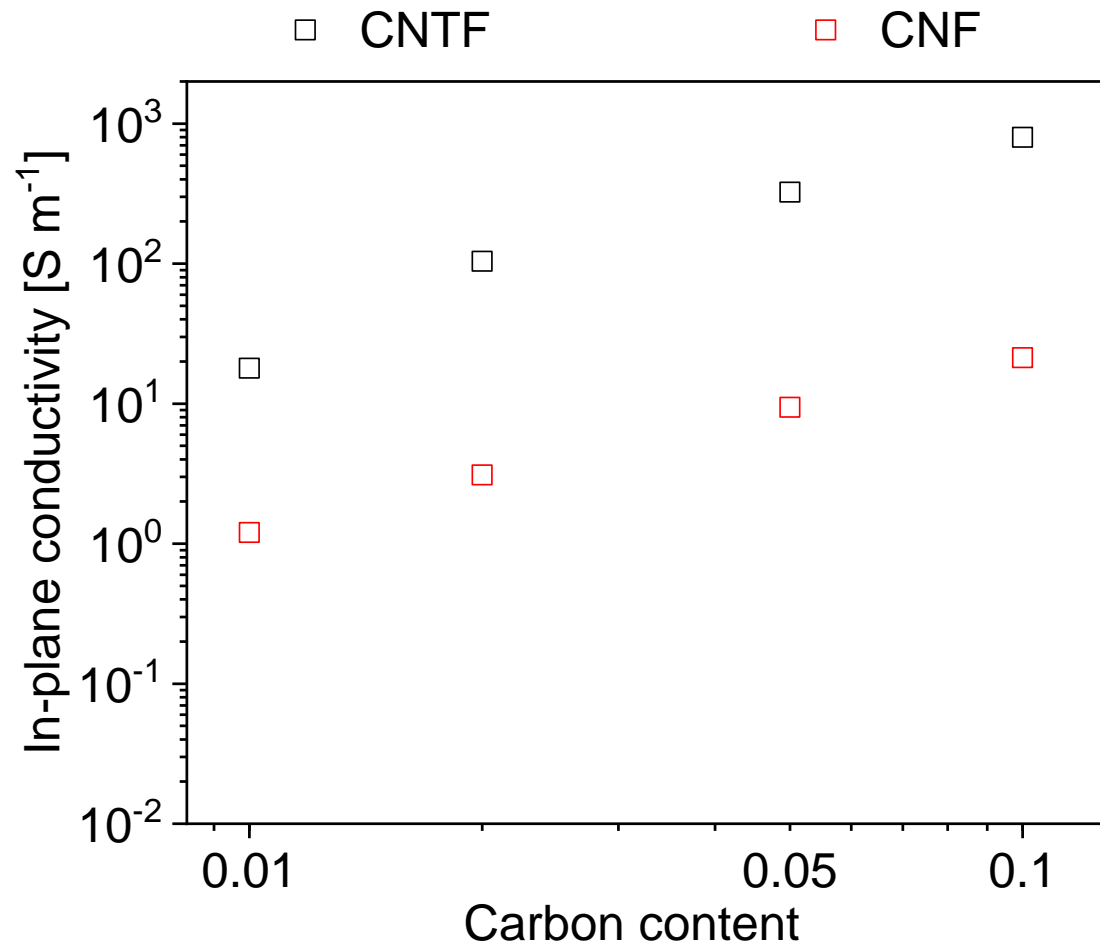


Figure S6 In-plane conductivity of PAN-derived CNF network and CNT embedded CNF (CNTF) network

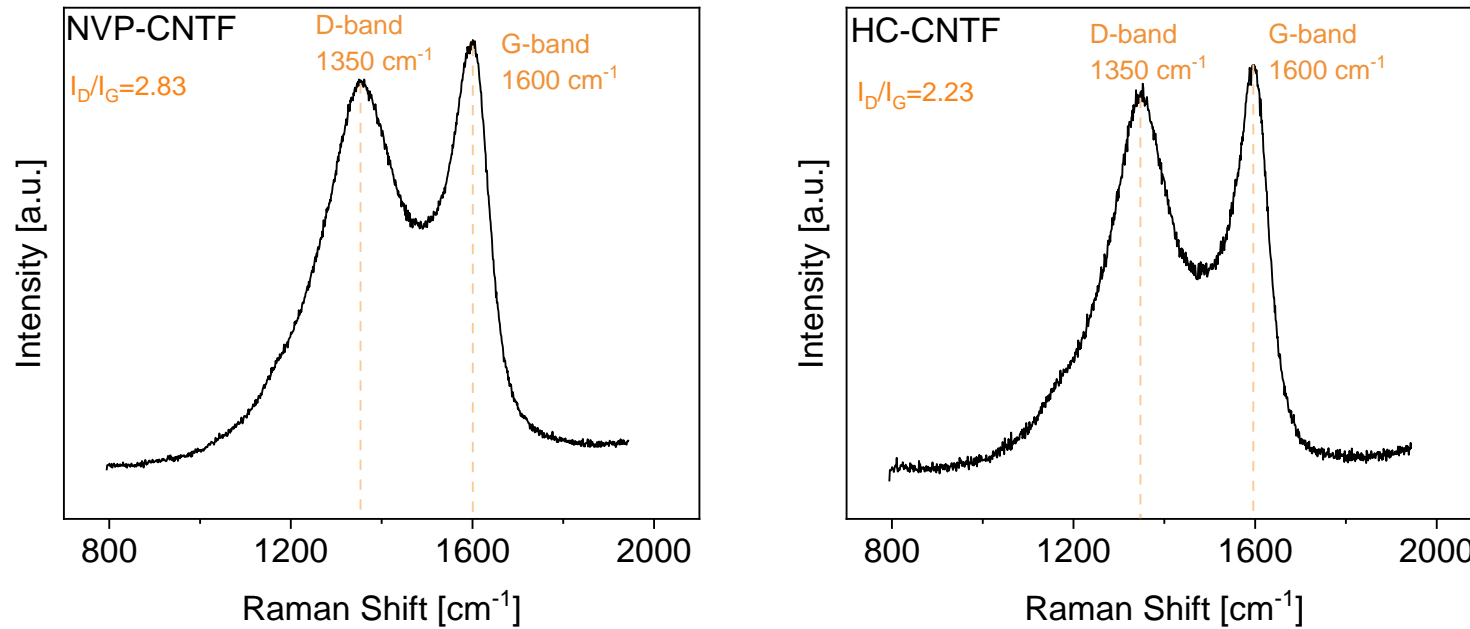


Figure S7 Raman spectrum of co-ESP NVPC/CNTF electrodes and HC/CNTF electrodes

The I_D/I_G value is inversely related to the degree of graphitisation of the carbon sample (Ferrari and Robertson 2000). The I_D/I_G values of NVPC-CNTF and HC-CNTF are 2.83 and 2.23, respectively. The lower I_D/I_G of the HC-CNTF is caused by its higher pyrolysis temperature (1100 vs. 850 °C). Both samples have lower I_D/I_G than previously reported PAN-derived carbon fibres pyrolyzed at same temperatures (Wang, Serrano et al. 2003). This is mainly due to the presence of CNT in the CNTF fibres(Bokobza and Zhang 2012).

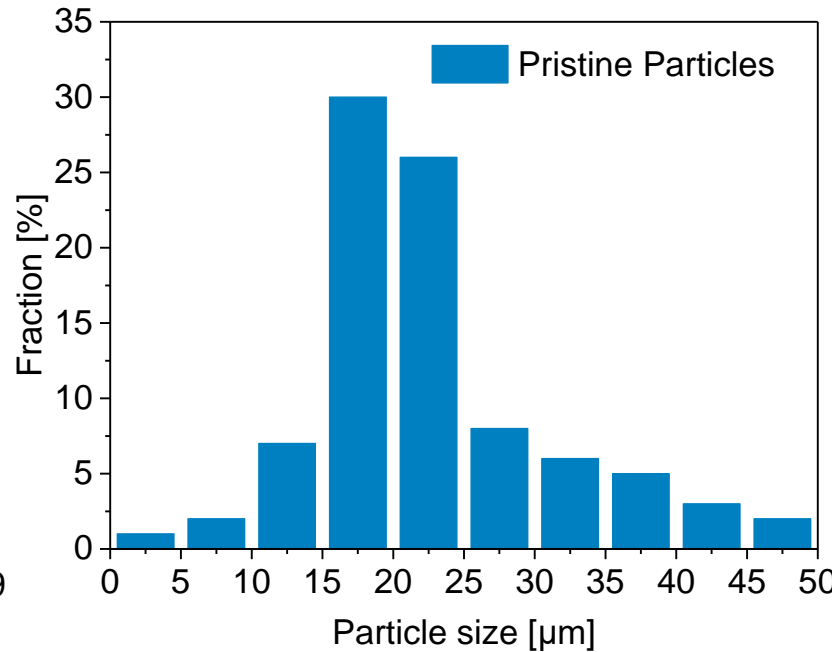
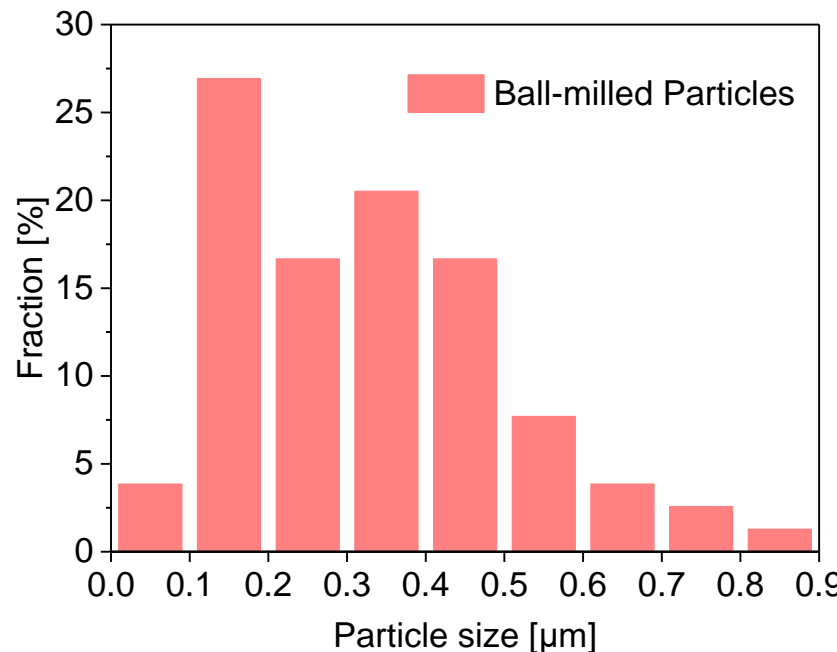


Figure S8 Particle size distribution of NVPC and ball-milled NVPC particles

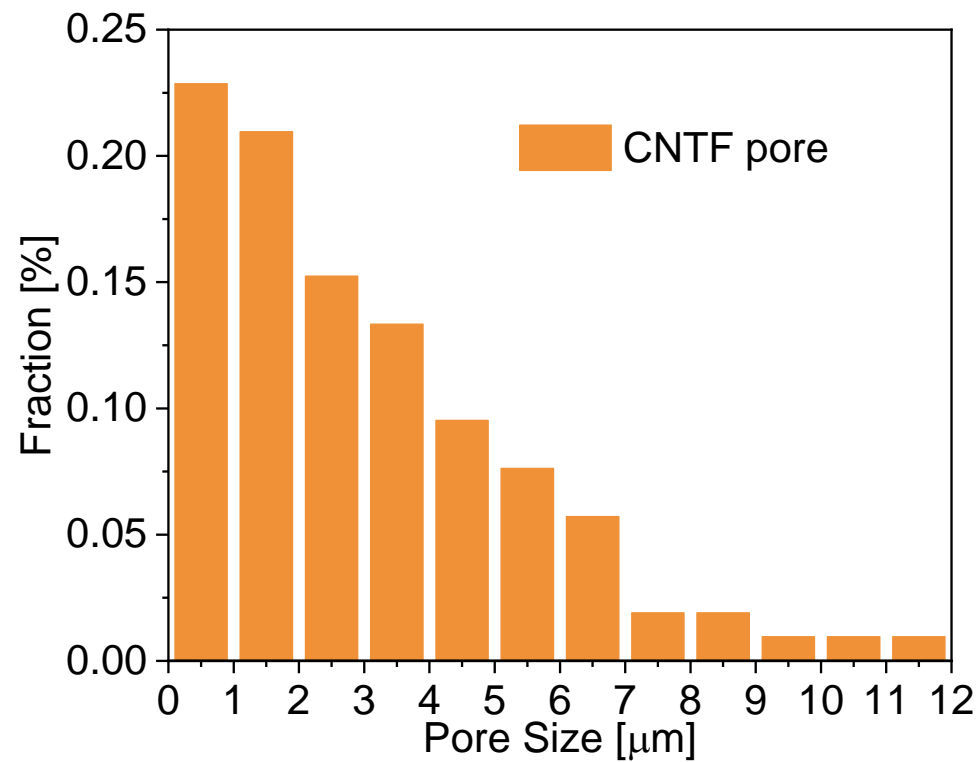


Figure S9 Pore size distribution of CNTF network

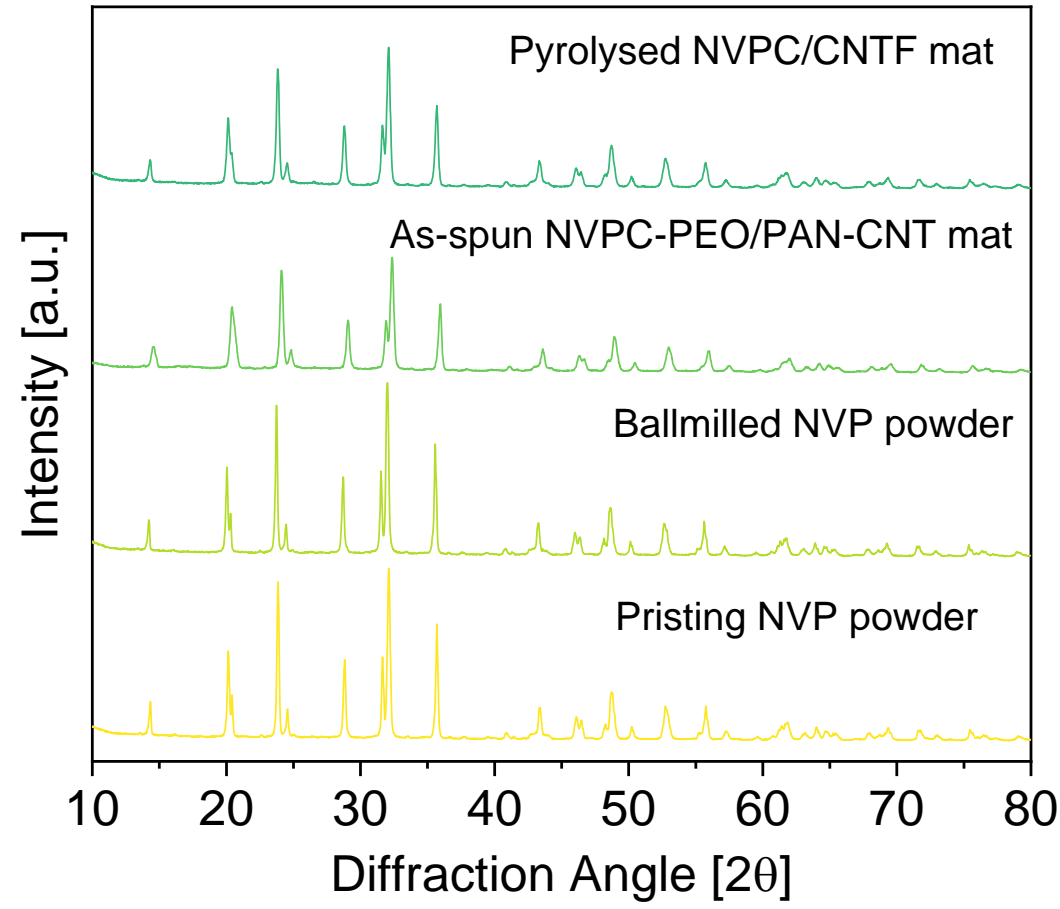


Figure S10 The X-ray diffraction (XRD) pattern of pristine and ball-milled NVPC particles and NVPC/CNTF electrode at different stages of preparation

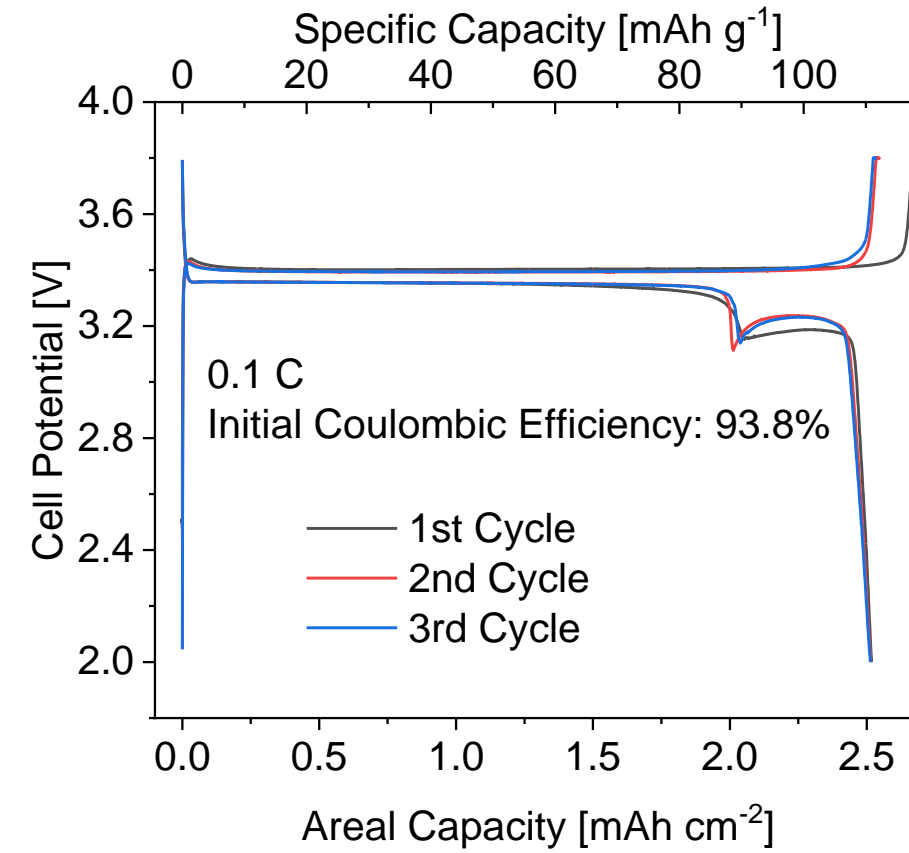
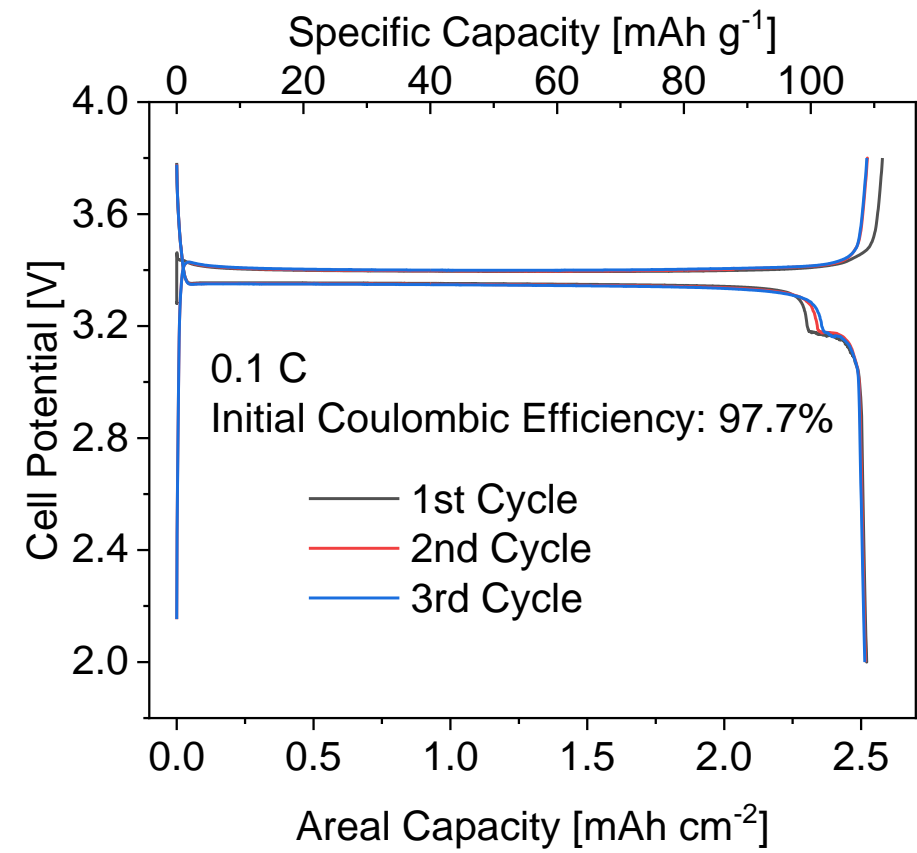


Figure S11 First three cycles of **a)** pristine and **b)** ball-milled NVPC/CNTF half cells

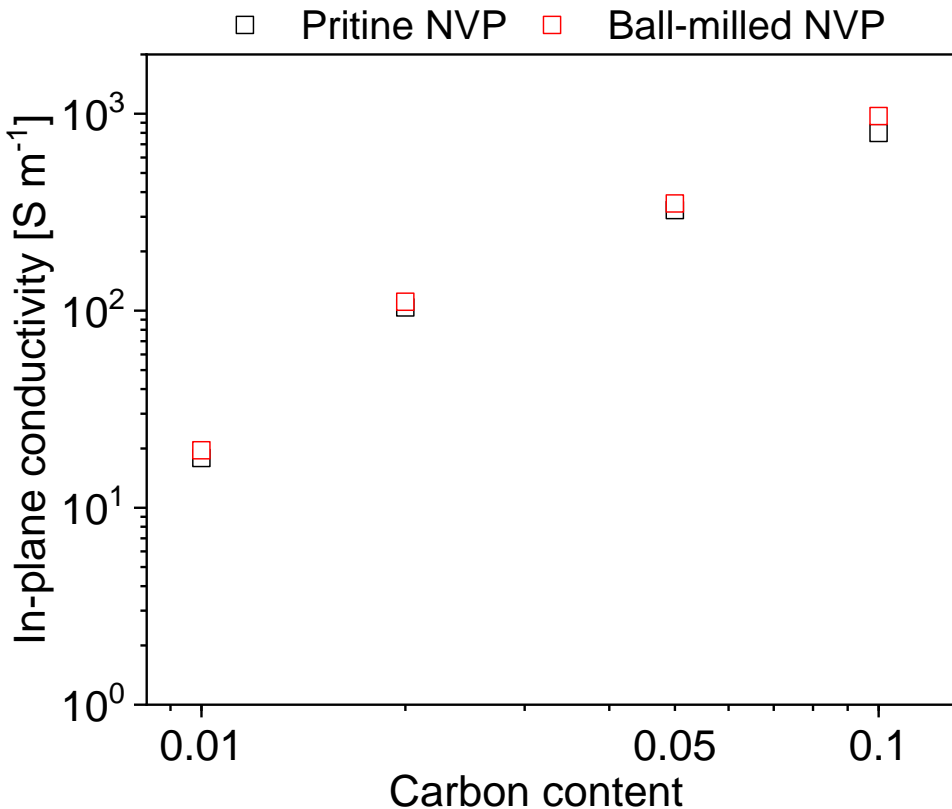


Figure S12 In-plane conductivity of co-ESP electrodes made by pristine NVPC and ball-milled NVPC

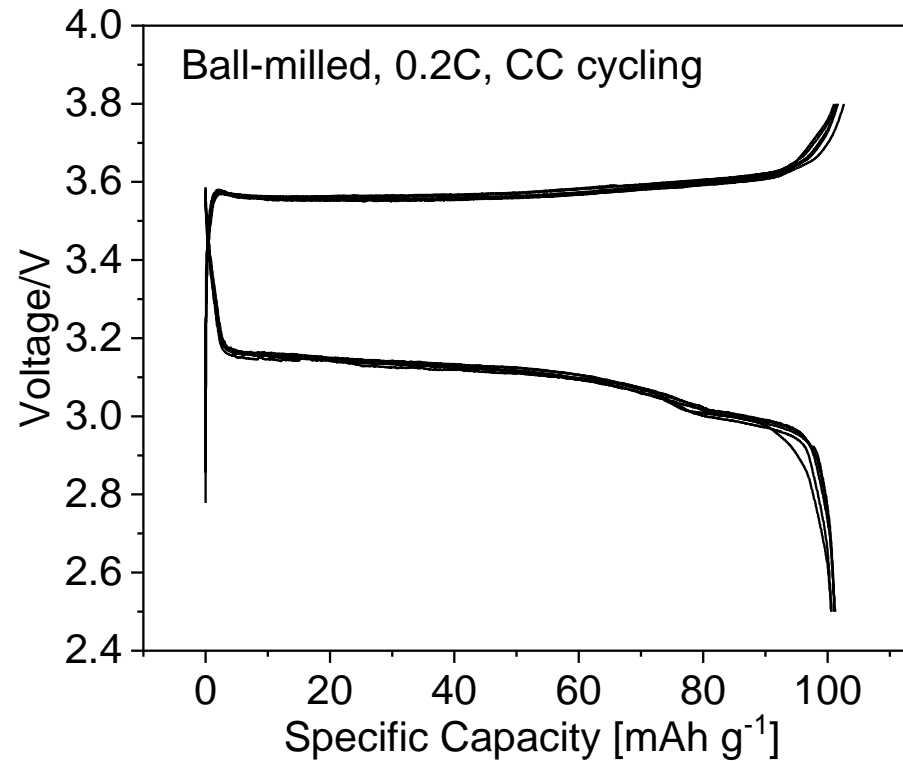
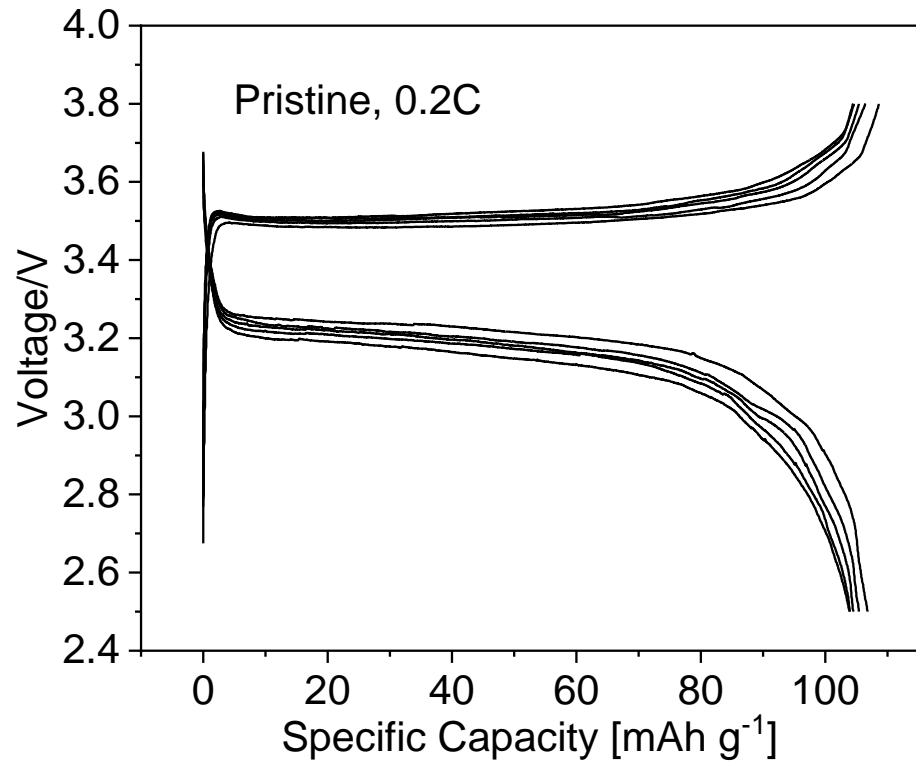


Figure S13 0.2C voltage profile of conventional slurry-casted electrode with pristine and ball-milled NVPC particles, CC cycling

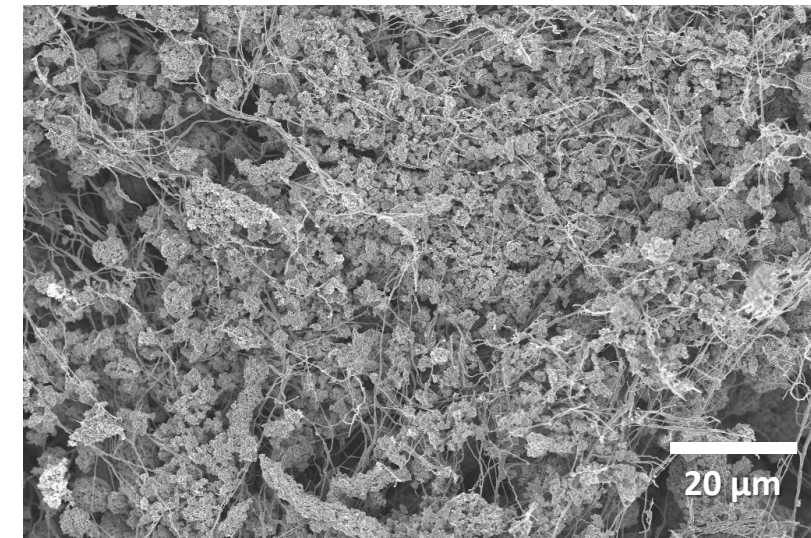
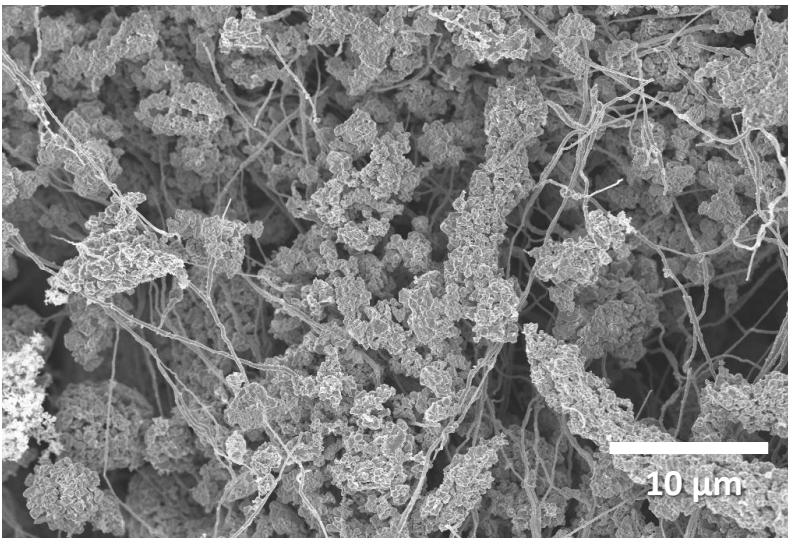
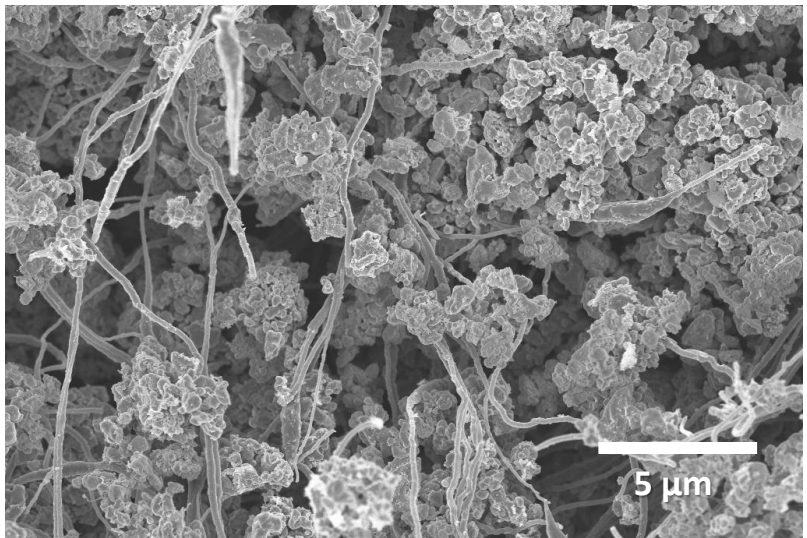
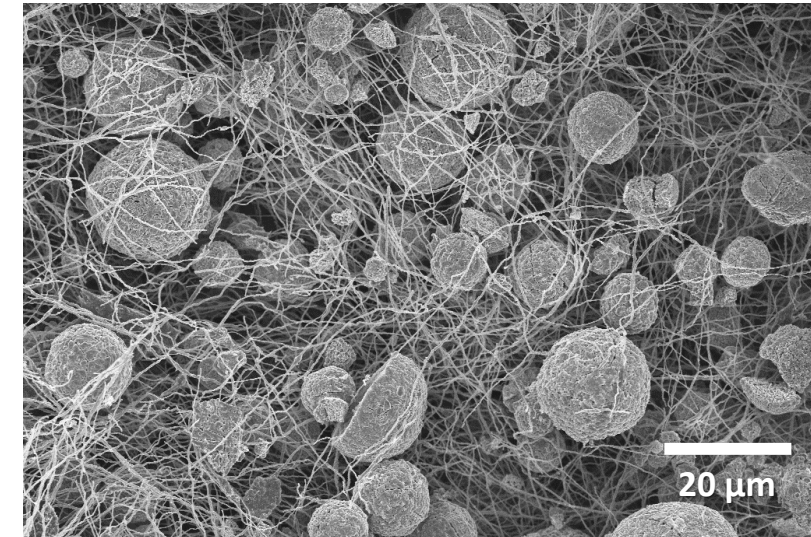
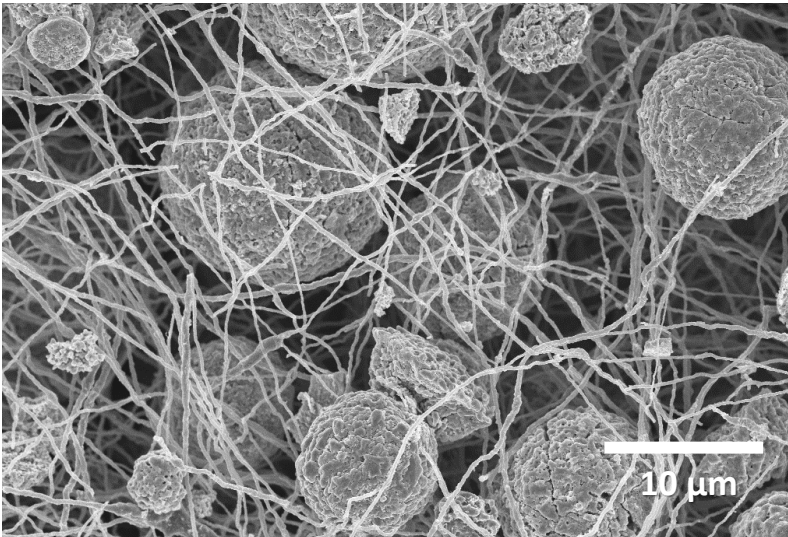
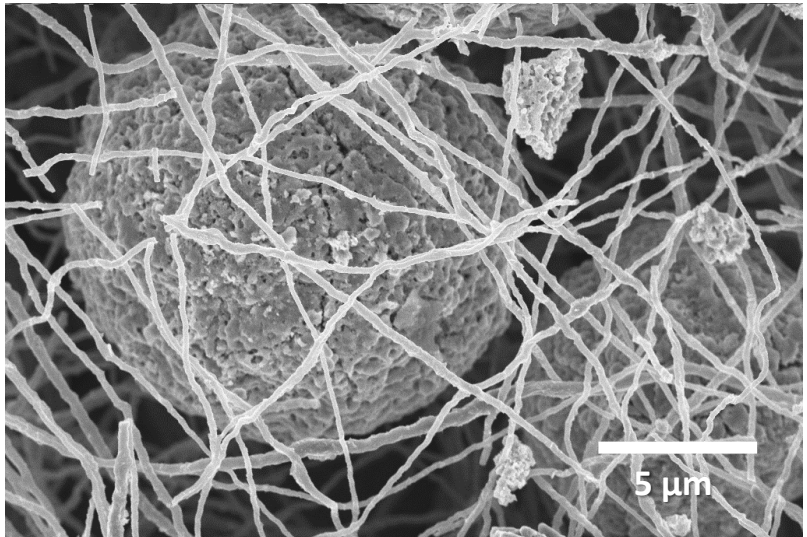
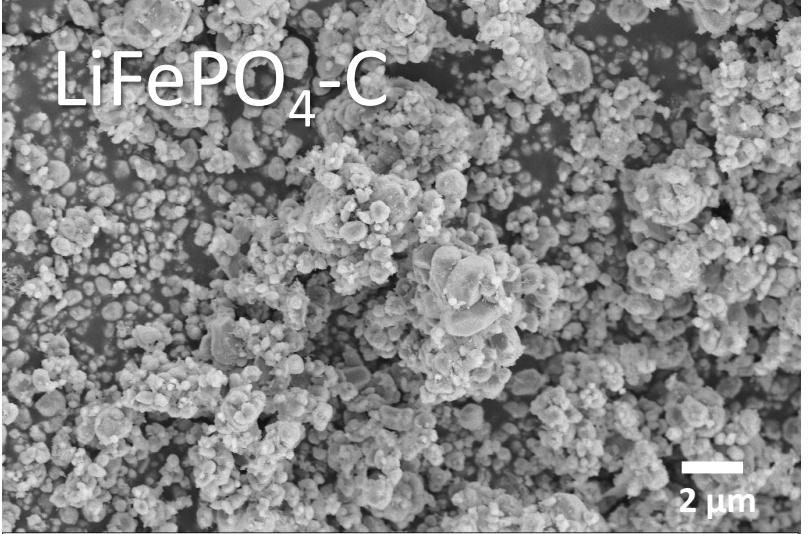
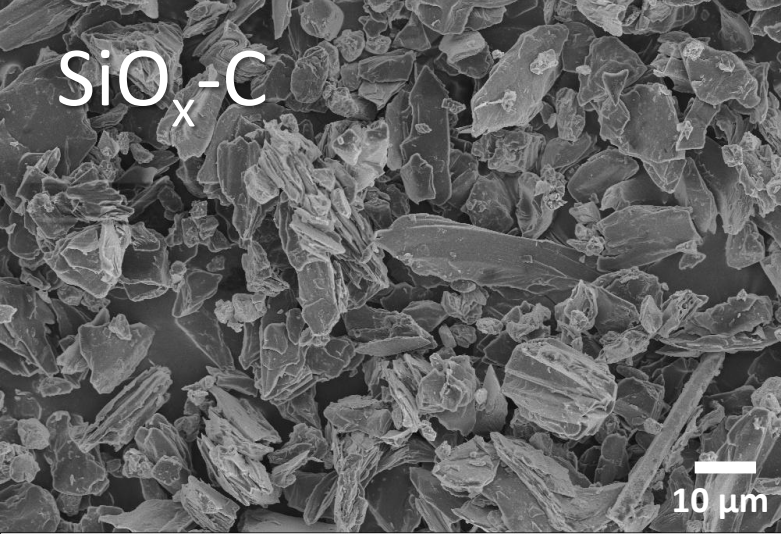


Figure S14 Photo/SEM images of co-ESP NVPC electrodes from **top**: pristine and **bottom**: ball-milled after 100 cycles (97.5wt% active content)

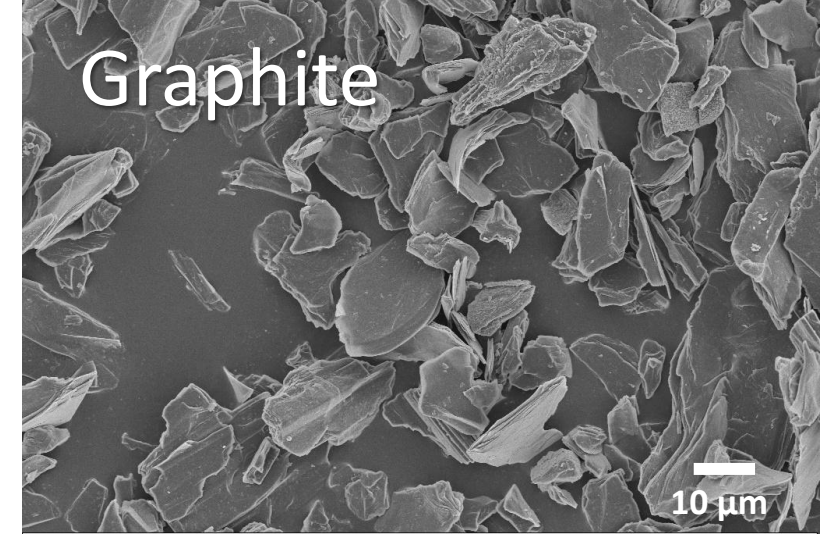
$\text{LiFePO}_4\text{-C}$



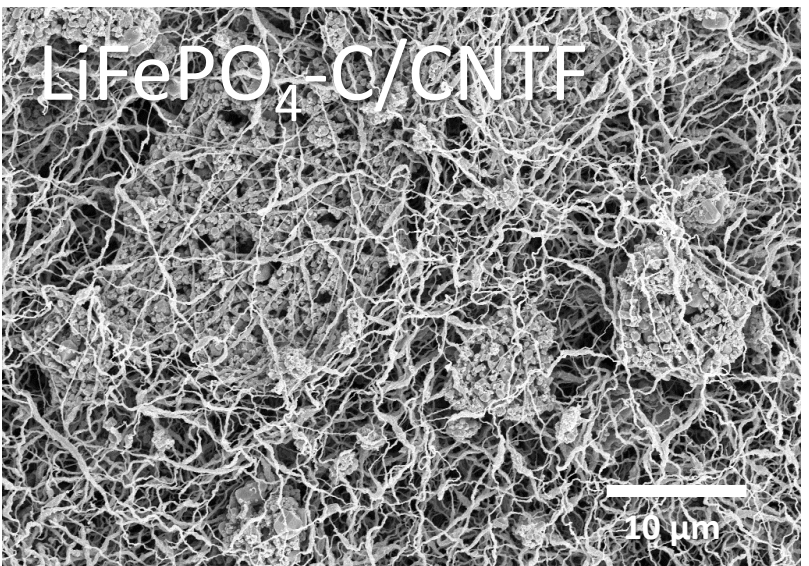
$\text{SiO}_x\text{-C}$



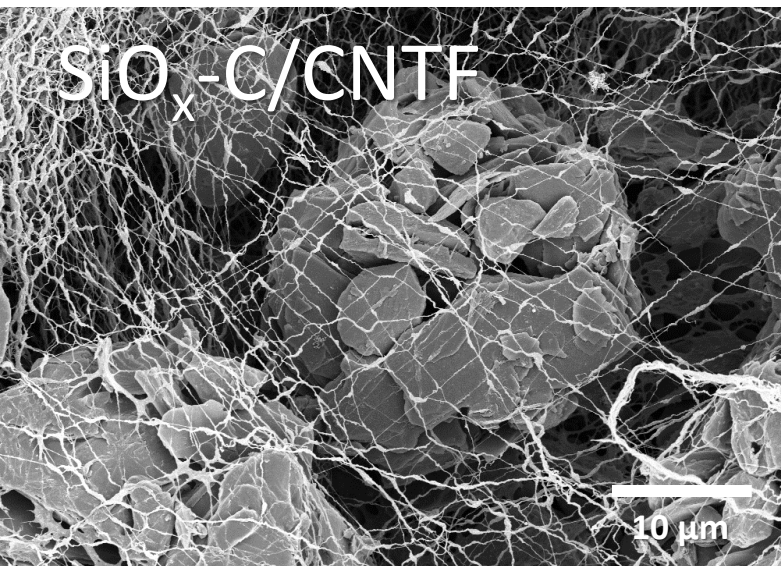
Graphite



$\text{LiFePO}_4\text{-C/CNTF}$



$\text{SiO}_x\text{-C/CNTF}$



Graphite/CNTF

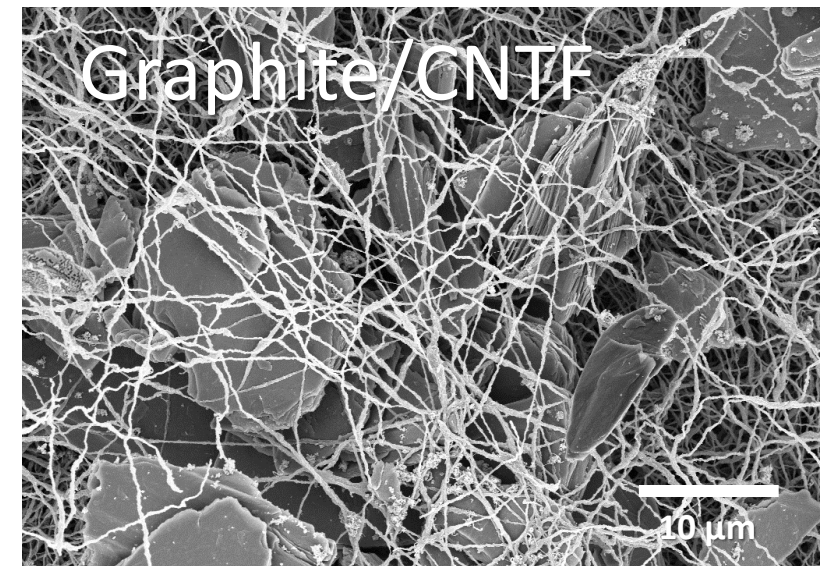


Figure S15 Morphologies of $\text{LiFePO}_4\text{-C}$, $\text{SiO}_x\text{-C}$ and graphite electrode produced by co-ESP method

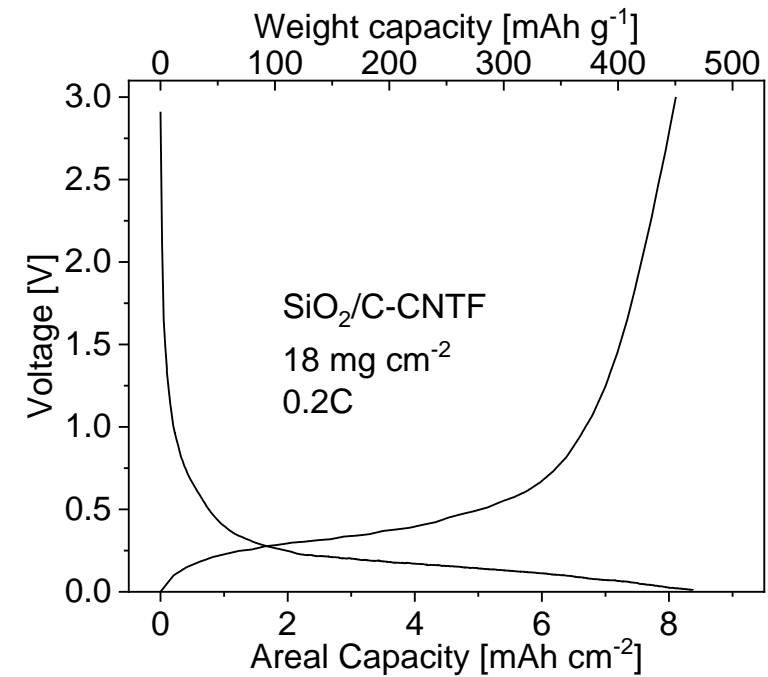
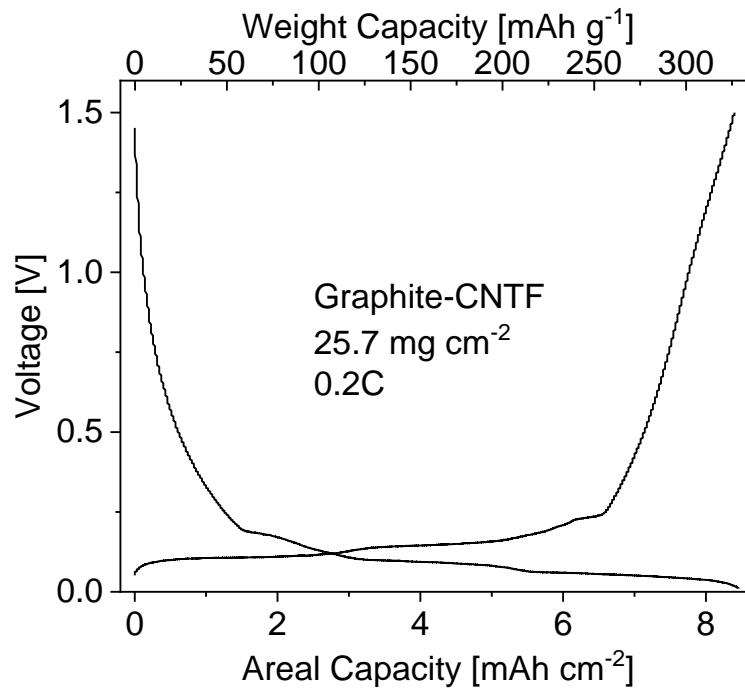
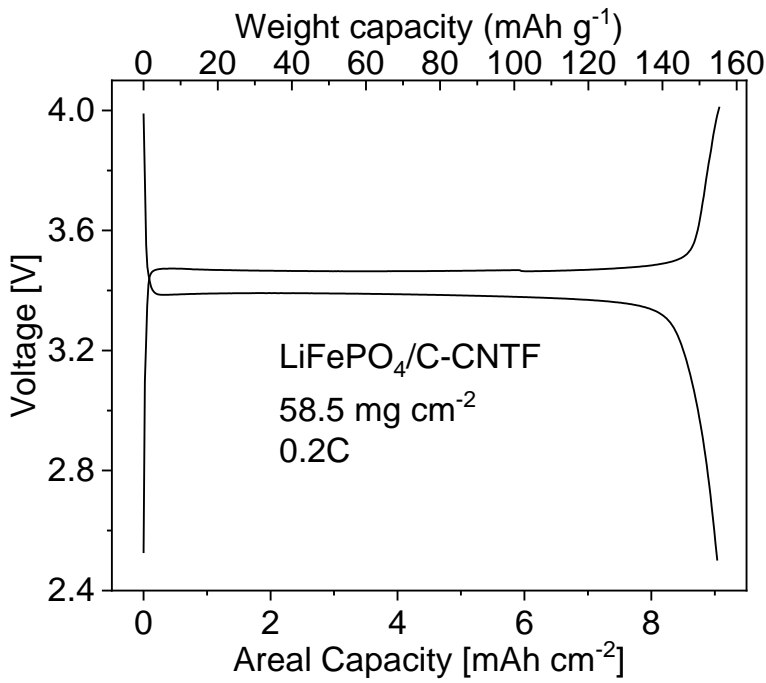


Figure S16 Voltage profiles of high areal loading LiFePO₄-C, graphite, and SiO_x-C electrode produced by co-ESP method

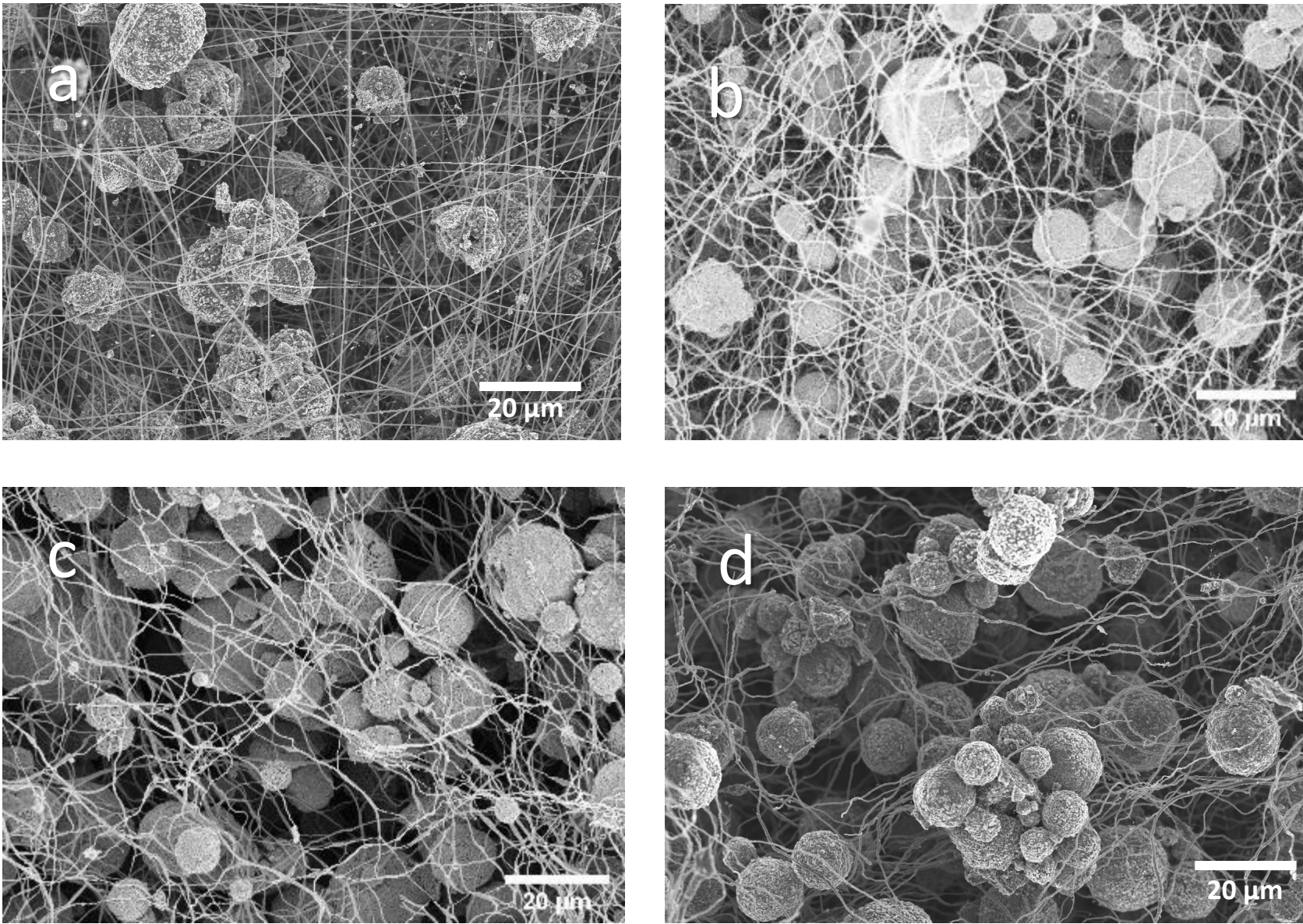


Figure S17 Morphology of NVPC/CNTF with a. 90 wt%; b. 97.5 wt%; c. 98 wt%; d. 99 wt% NVPC content

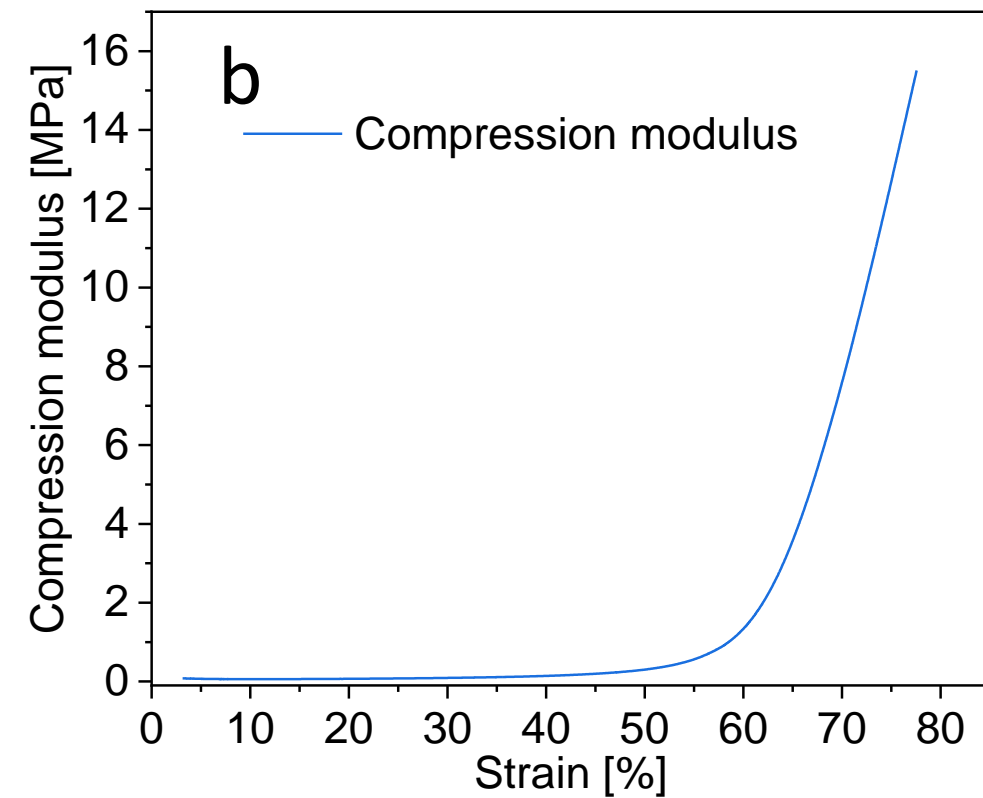
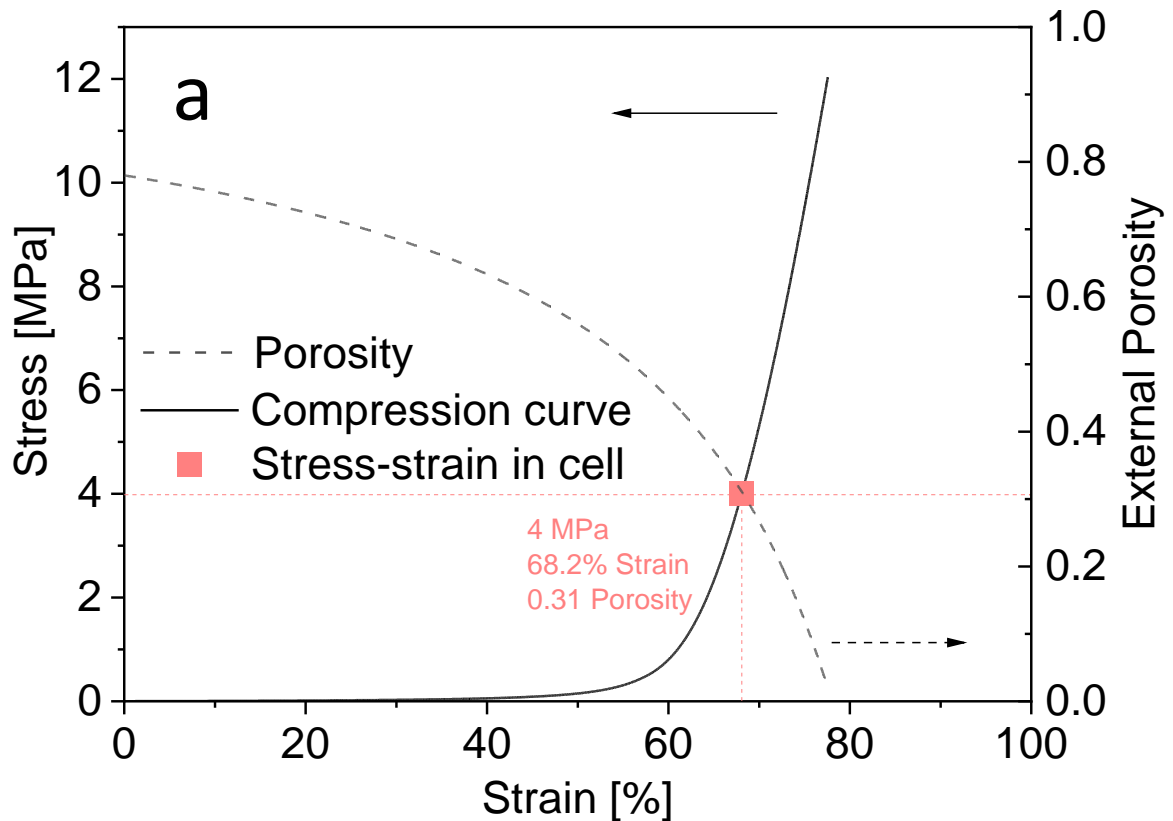


Figure S18 a) The relation of stress, strain and external porosity of the NVPC/CNTF electrodes; **b)** the compression modulus vs. strain of the co-ESP electrode.

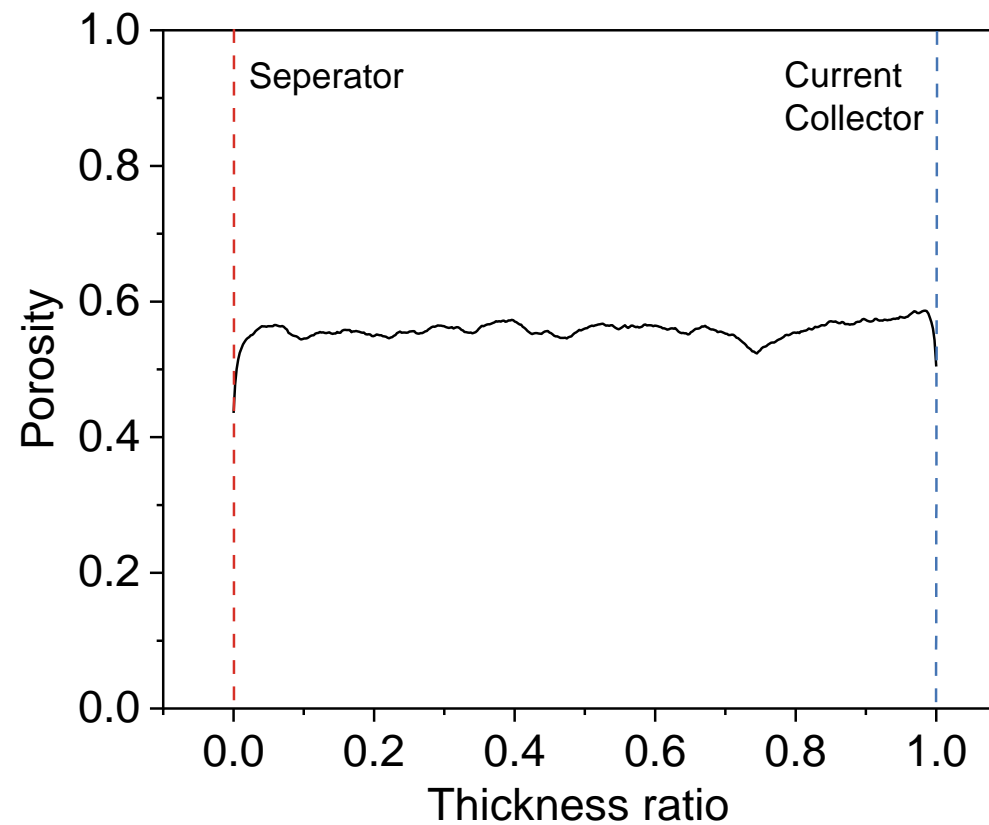


Figure S19 Uniformity of porosity across thickness

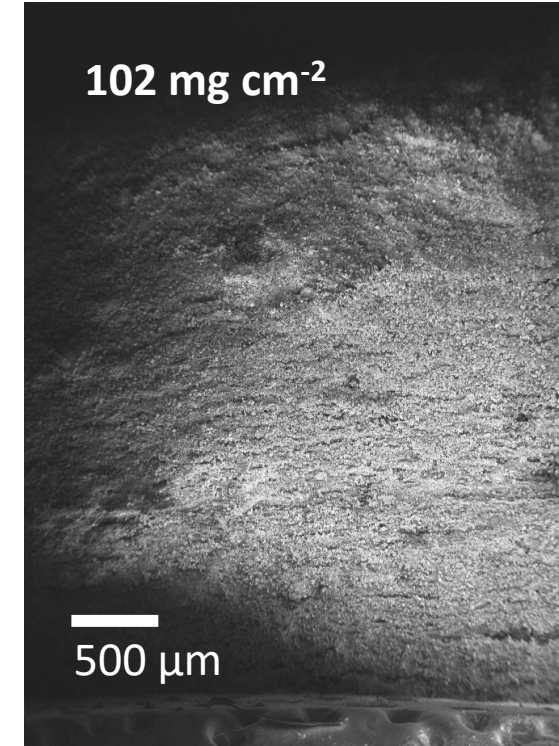
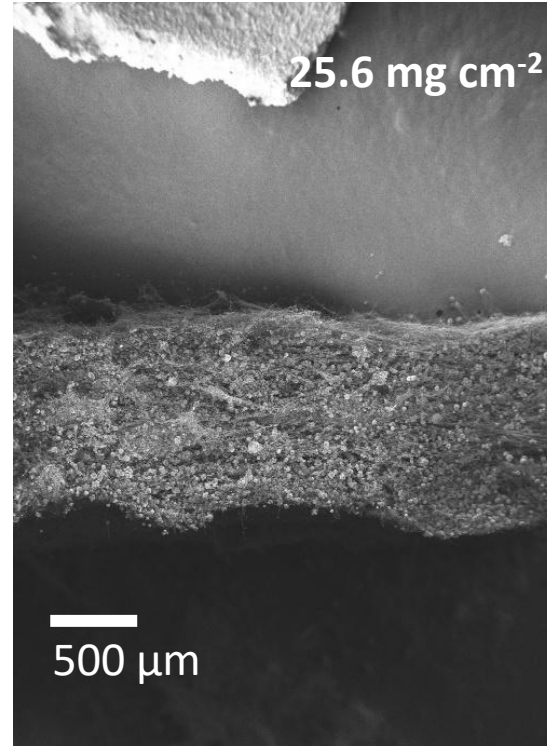
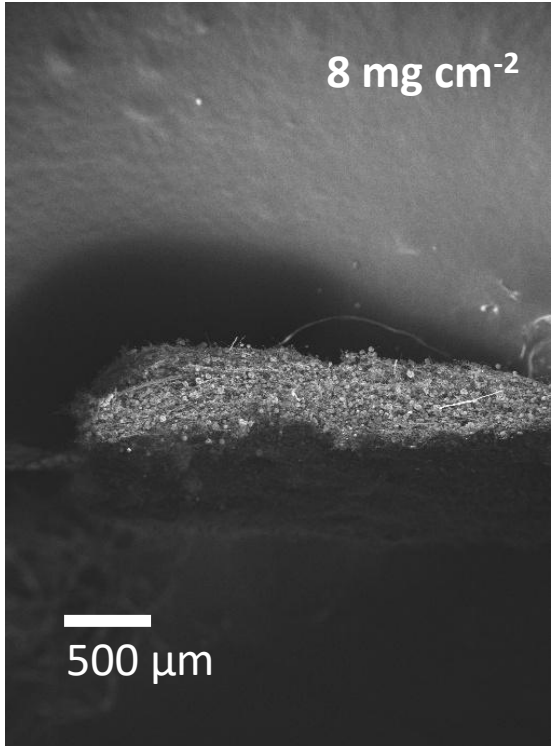


Figure S20 Cross-section morphologies of co-ESP NVPC/CNTF electrodes of different areal loadings, uncompressed.
Left to right: 8 mg cm^{-2} , 25.6 mg cm^{-2} , 102 mg cm^{-2}

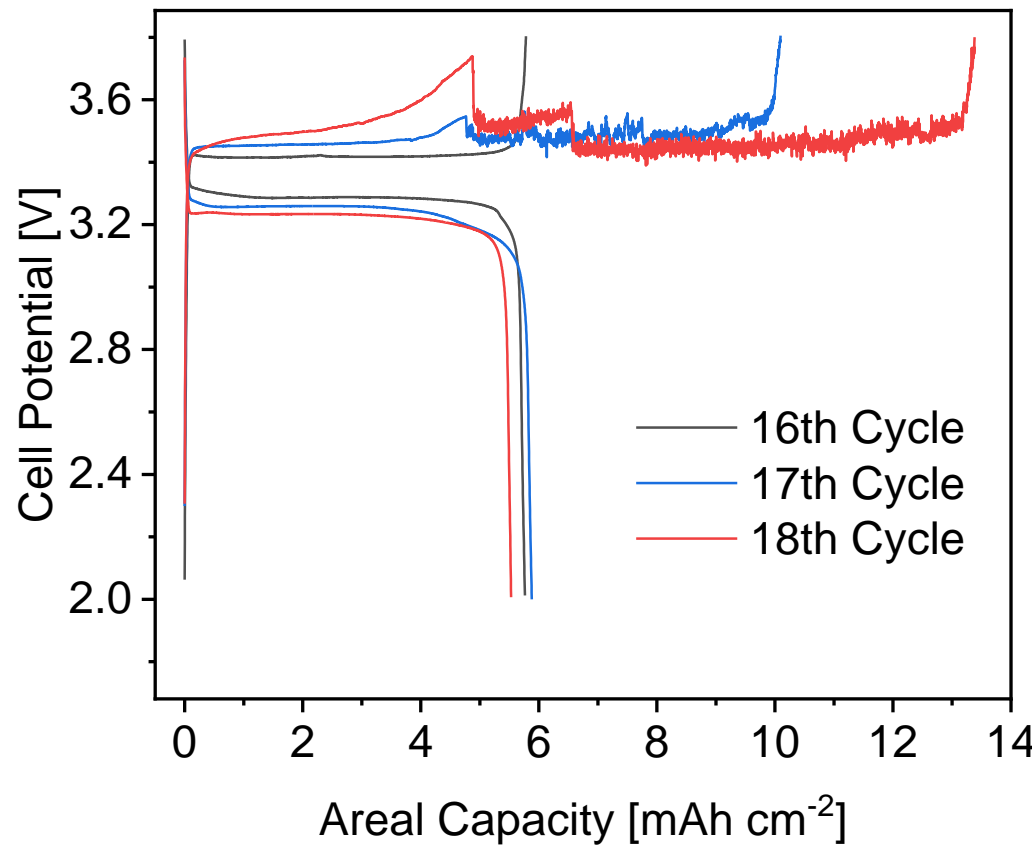


Figure S21 16-18th cycles of NVPC/CNTF half cells with FEC 56.7 mg cm^{-2} , the overcharging started from the 17th cycle in this cell even FEC is added in the electrolyte.



Figure S22 Sodium anode after overcharging in a NVPC/CNTF half-cell with 60.7 mg cm^{-2} areal loading, 20 cycles in total.

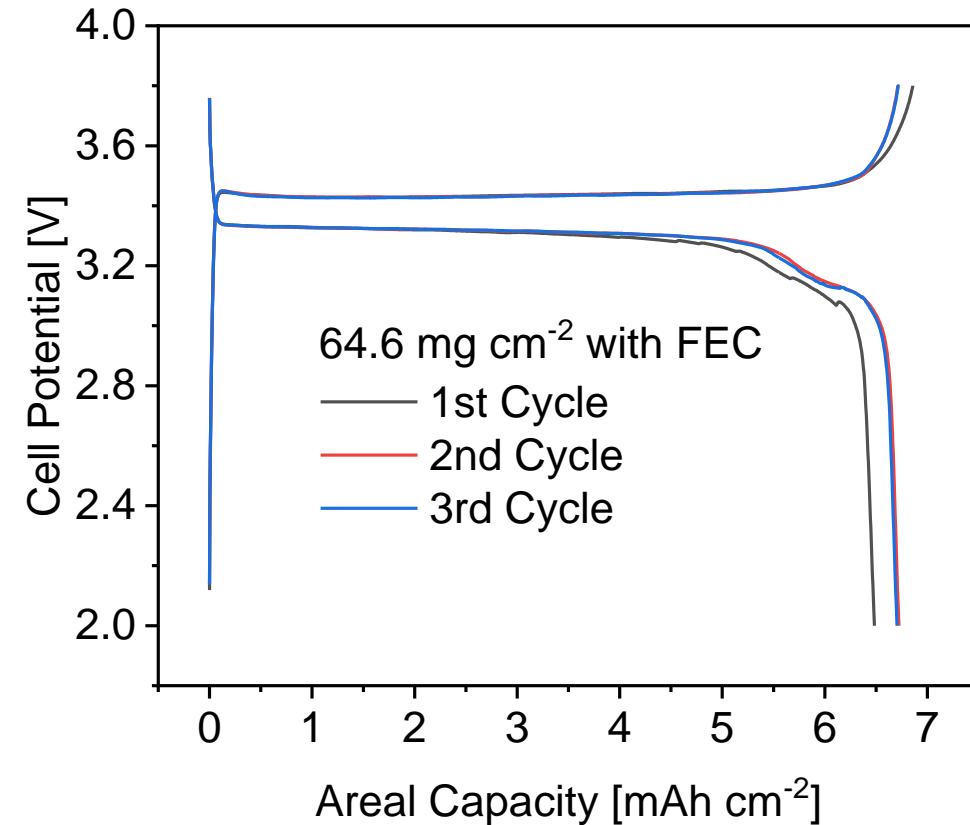
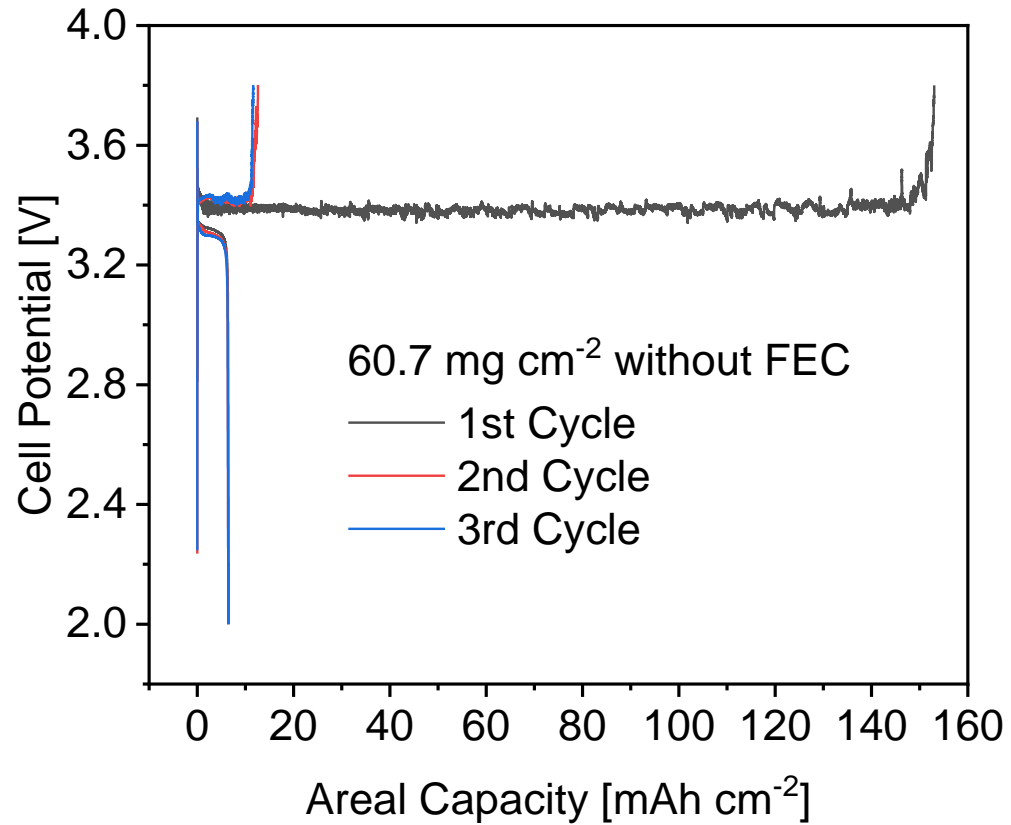
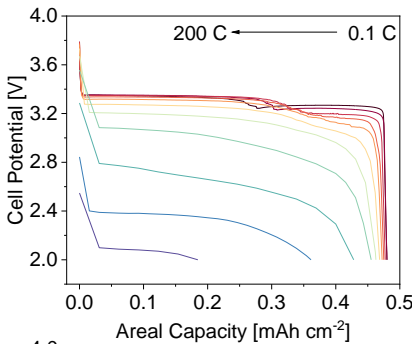
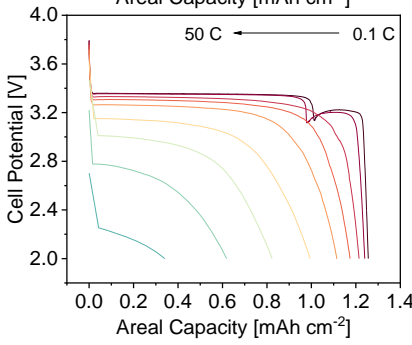


Figure S23 First three cycles of NVP/CNT-CNF half cells without FEC 60.7 mg cm⁻² or with FEC 64.6 mg cm⁻²

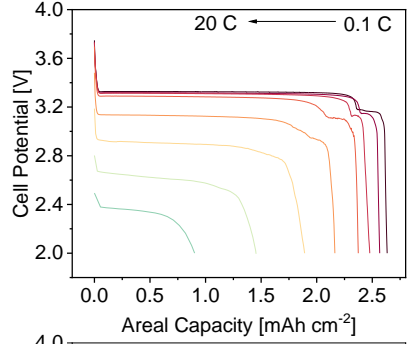
4.3 mg cm^{-2}



11.3 mg cm^{-2}



23.9 mg cm^{-2}



49.6 mg cm^{-2}

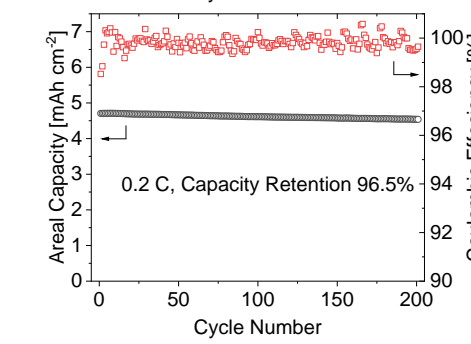
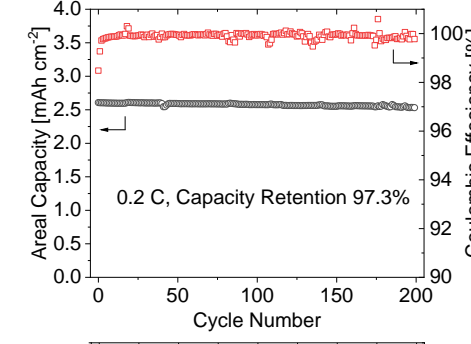
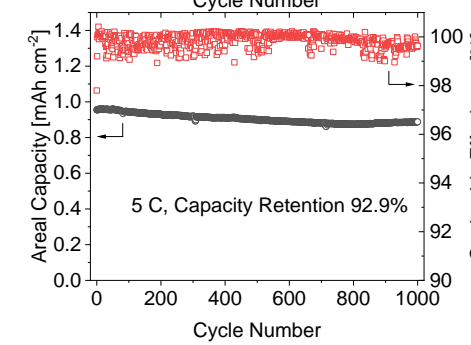
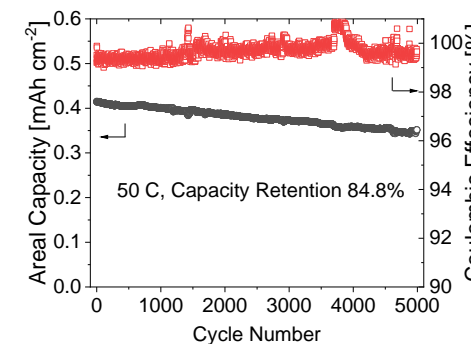
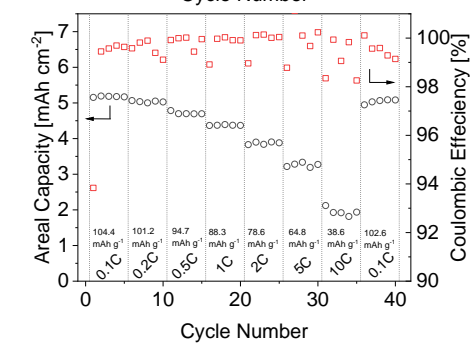
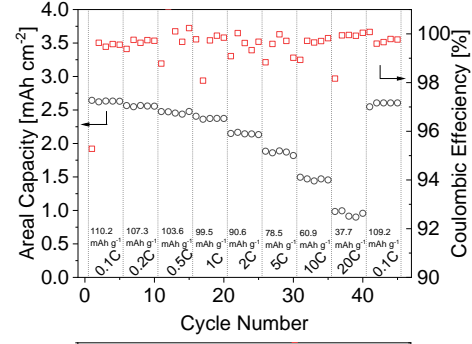
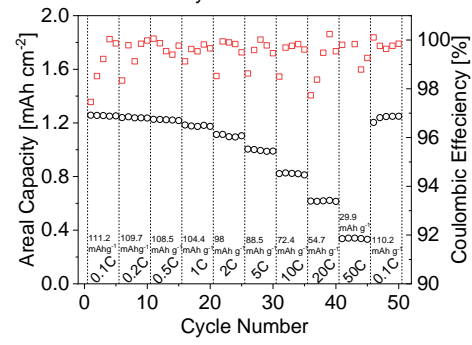
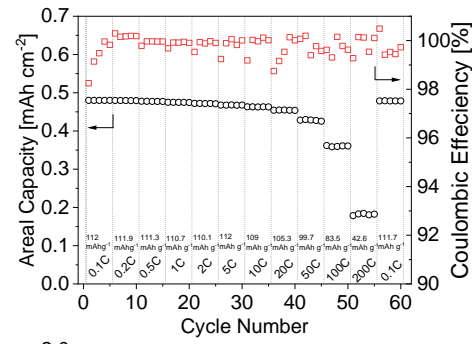
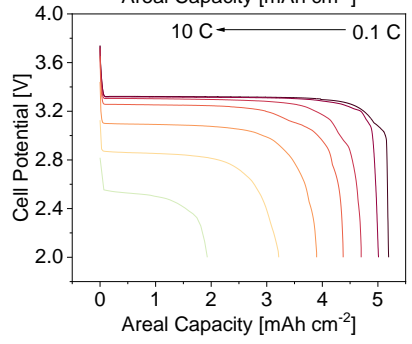


Figure S24 Cycling data of NVP/CNTF half cells of different areal loading

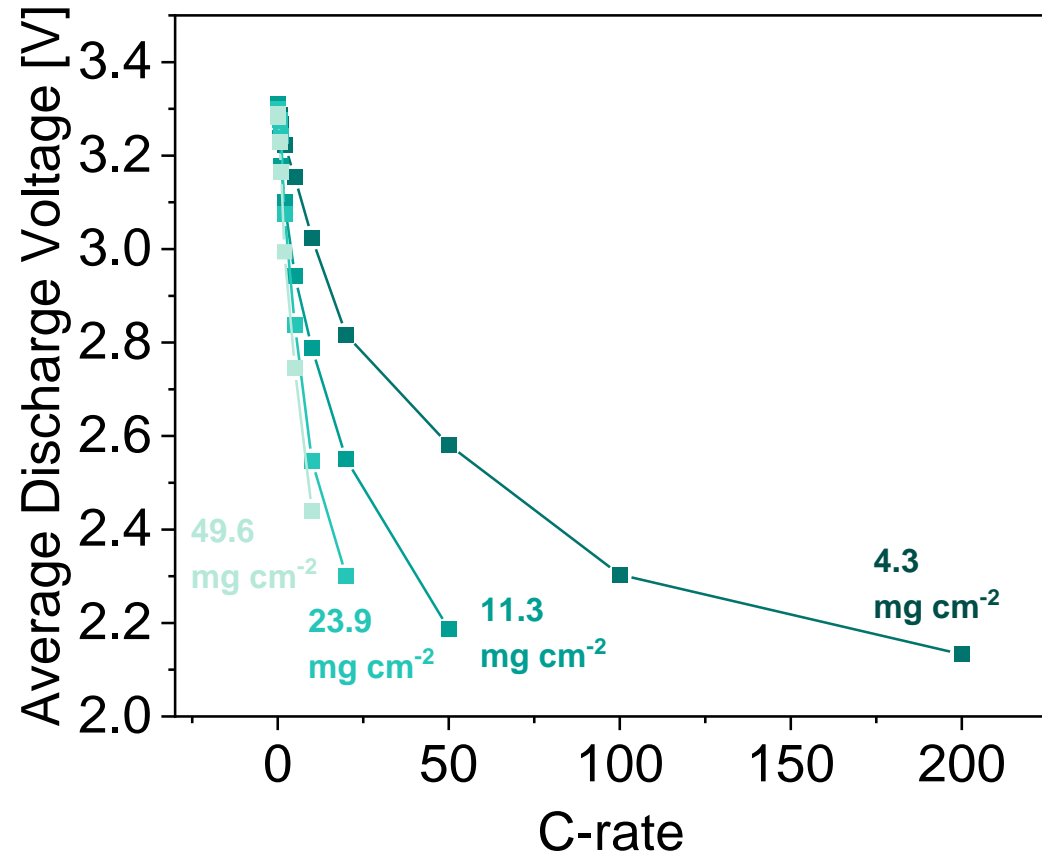


Figure S25 Average discharge voltage of co-ESP NVPC half-cells of different areal loading and C-rate

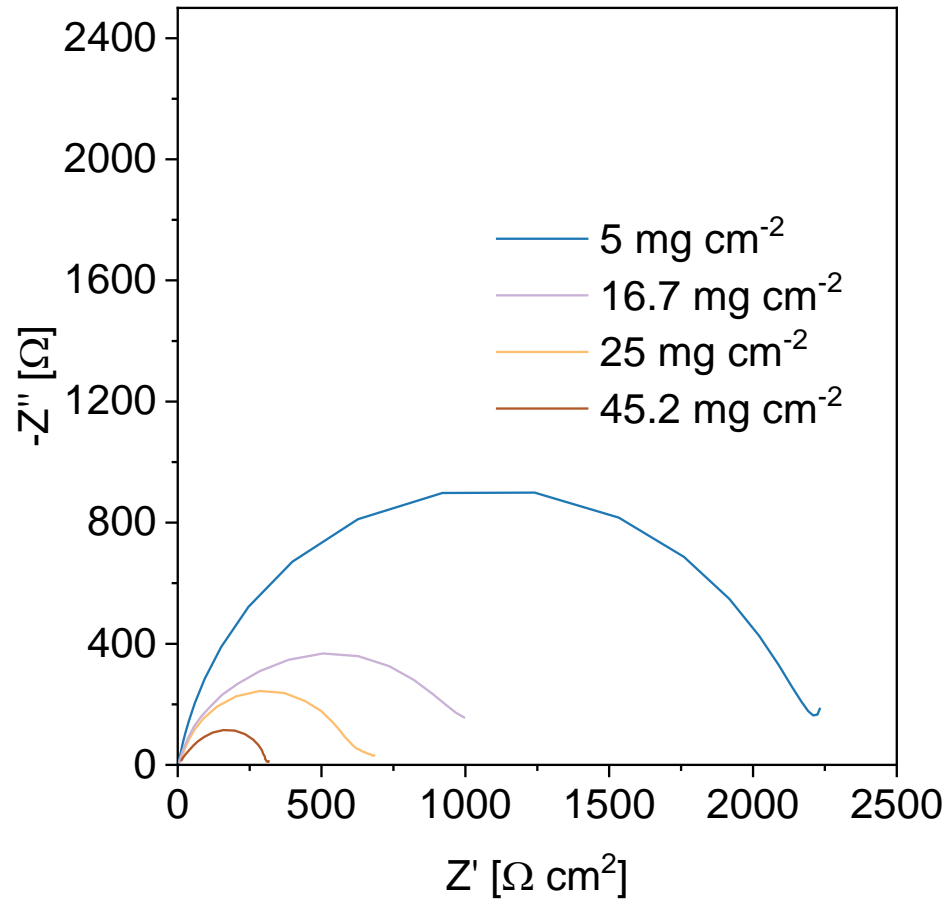


Figure S26 Nyquist of NVP/CNTF half cell of different loading, 0% state of charge

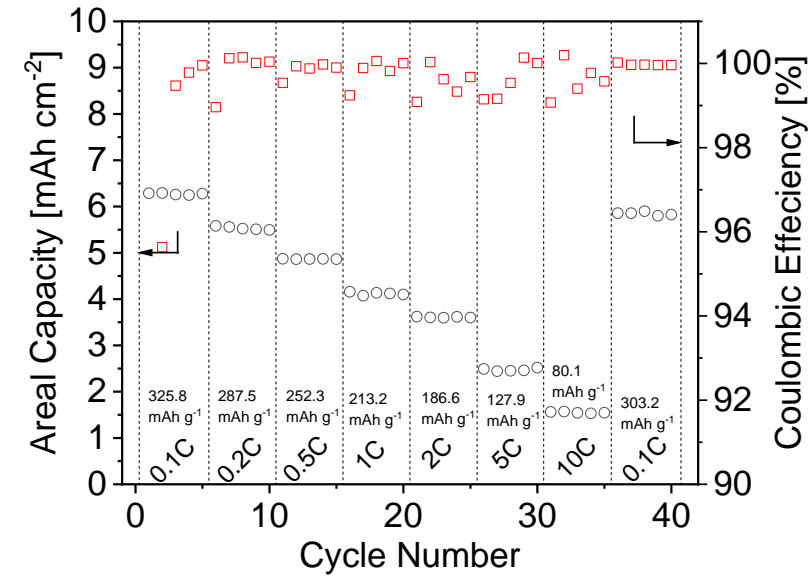
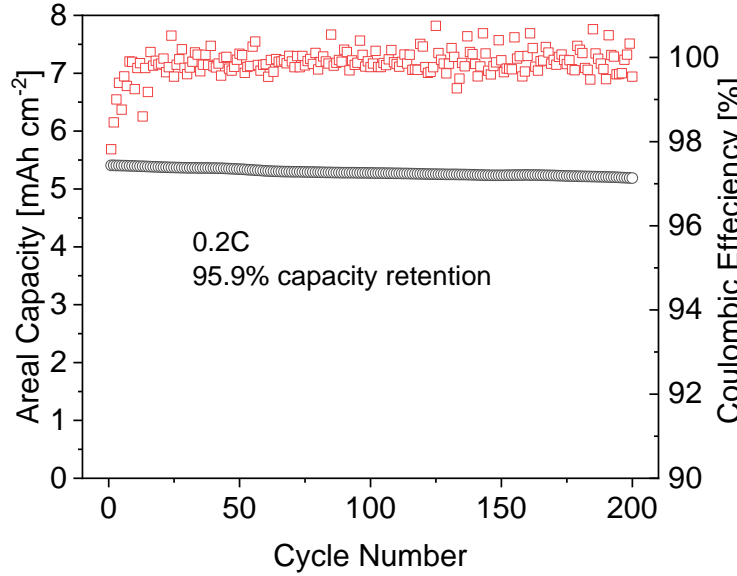
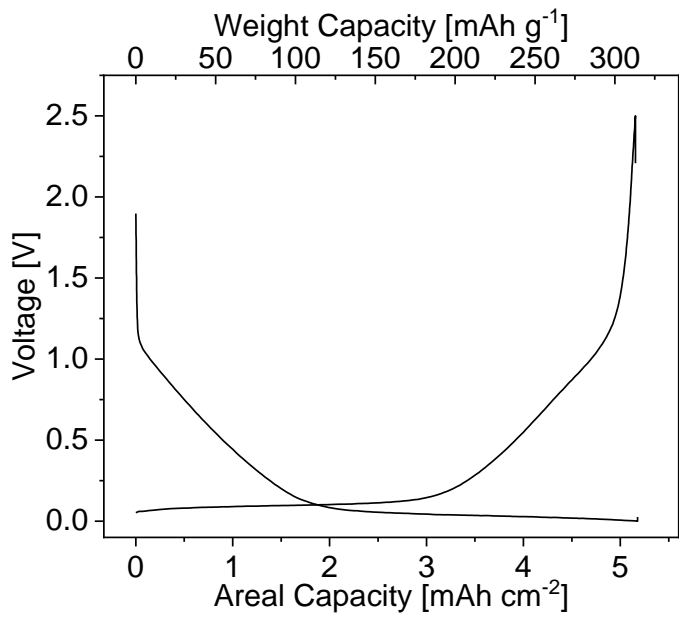


Figure S27 Voltage profile (left), cycling stability (middle) and rate performance (right) of glucose-derived hard carbon half cells. left, middle: areal loading 16.5 mg cm^{-2} , 0.2C; Right: 13.5 mg cm^{-2}

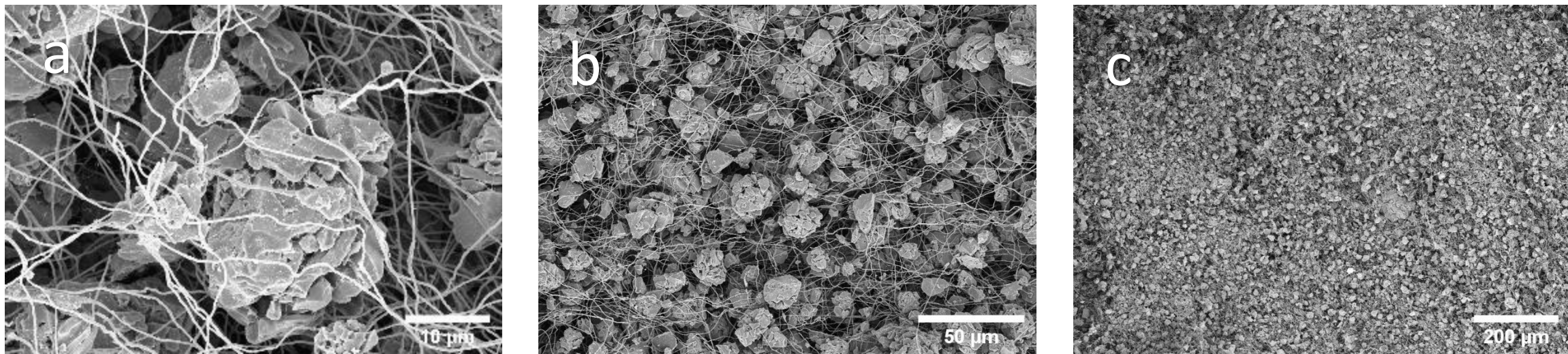


Figure S28 Morphology of co-ESP hard carbon/CNTF electrodes

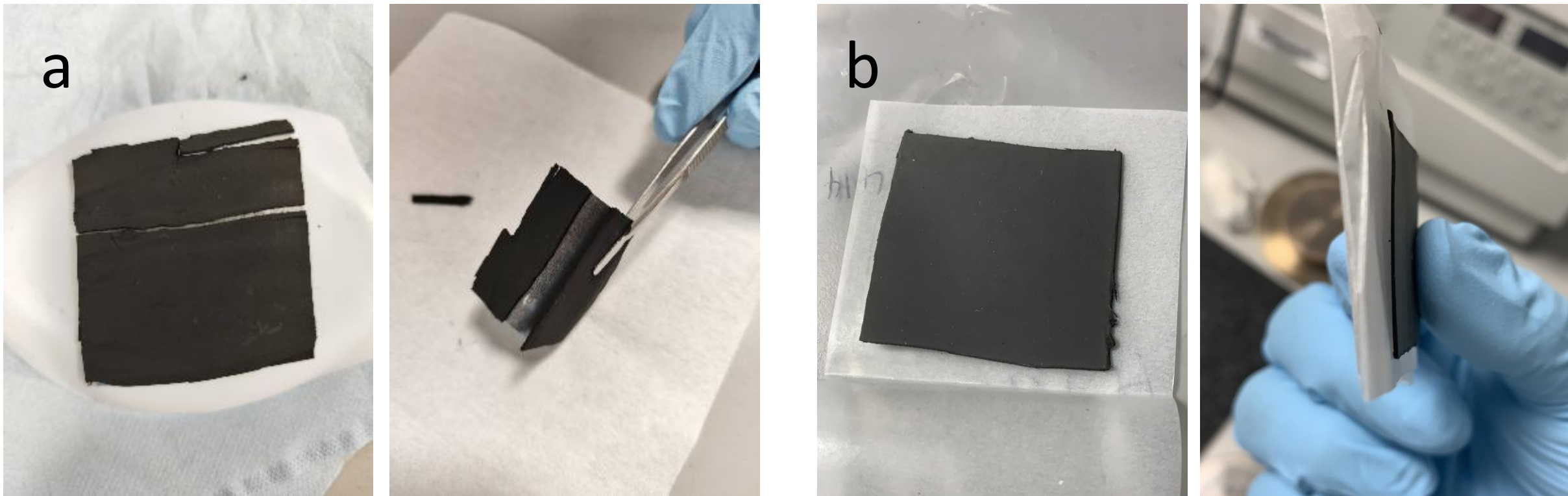


Figure S29 Photos of **a.** cracked and delaminated conventional NVPC electrodes with 80 mg cm^{-2} areal loading; **b.** compressed 100 mg cm^{-2} co-ESP NVPC/CNTF pouch cell electrode

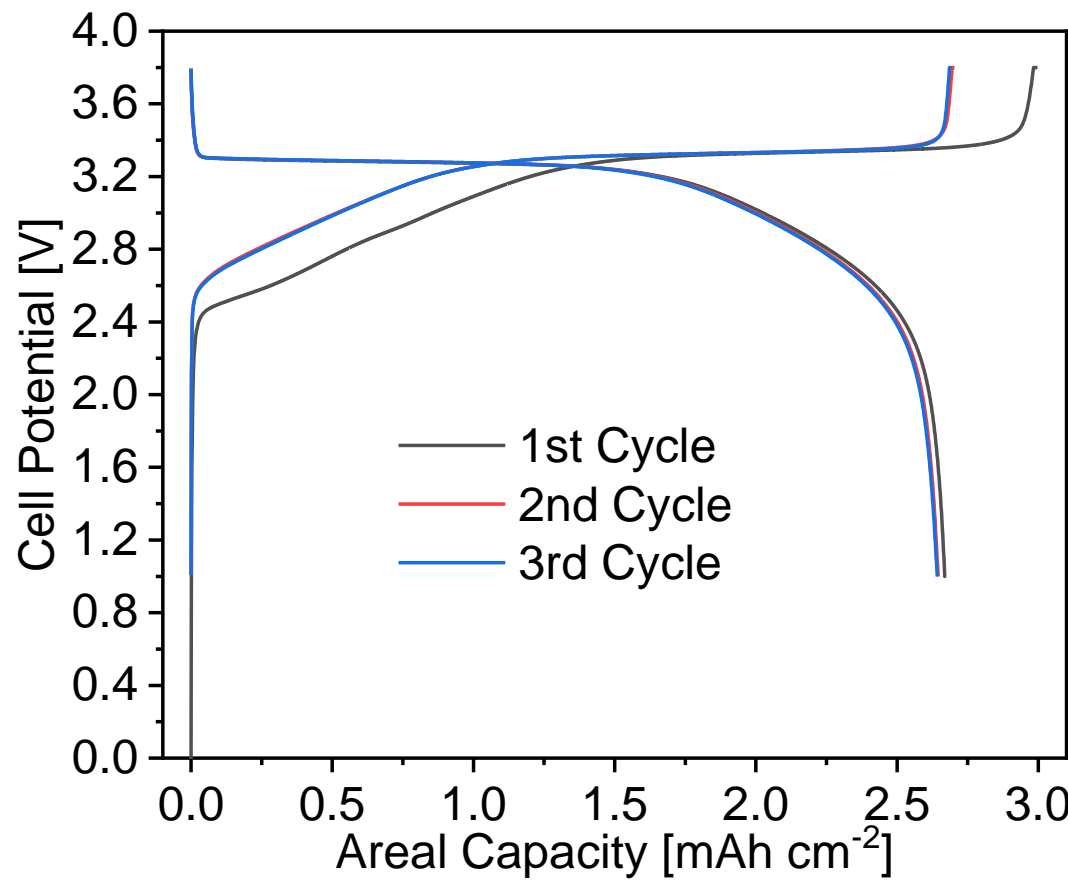
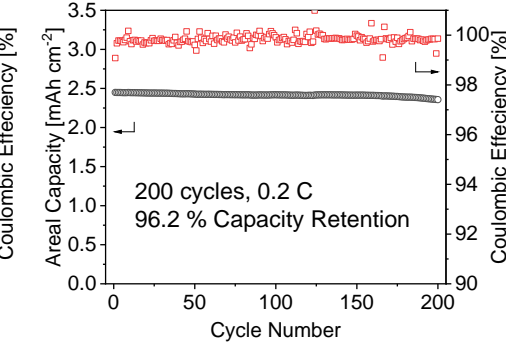
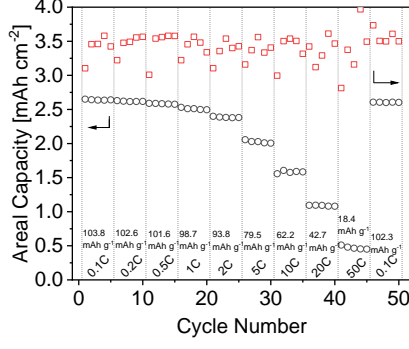
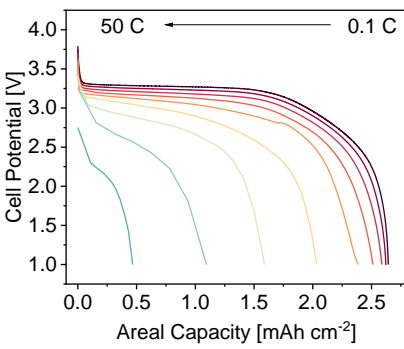
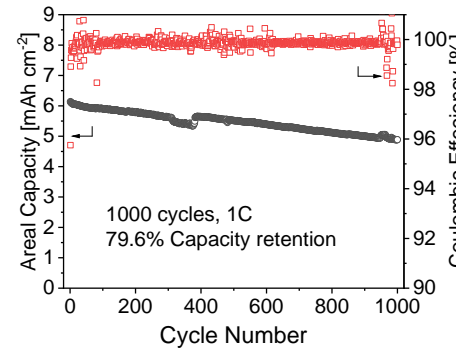
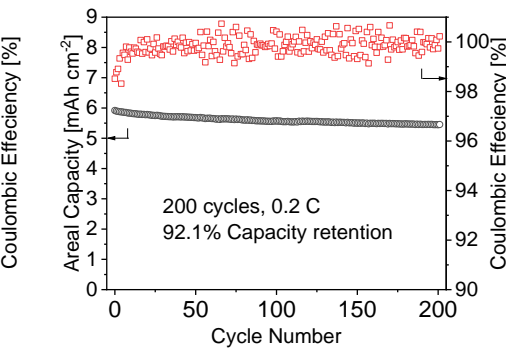
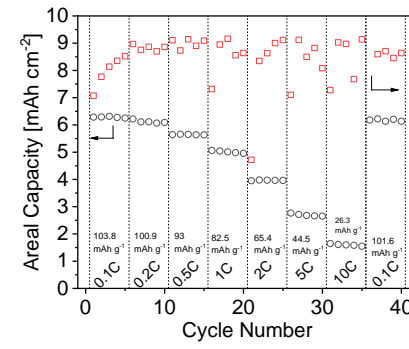
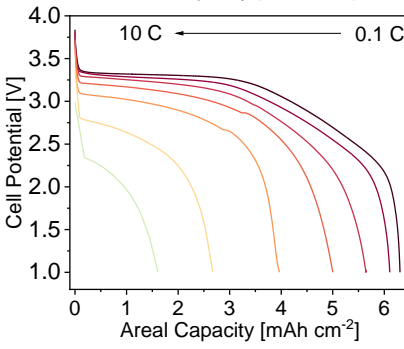


Figure S30 First three cycles of co-ESP NVPC/CNTF full cells with 25.4 mg cm^{-2} areal loading

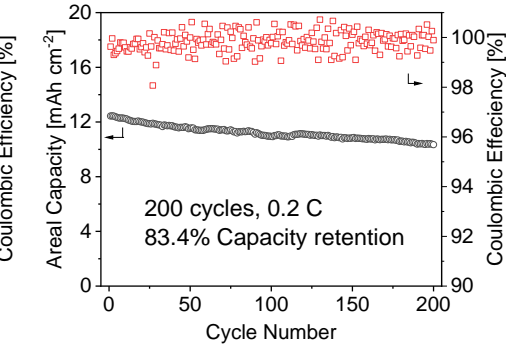
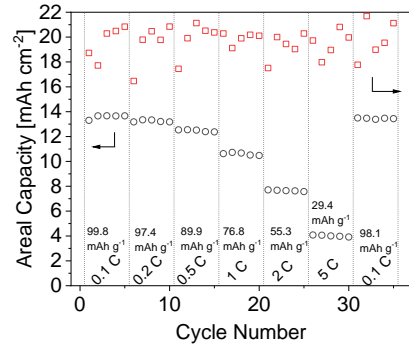
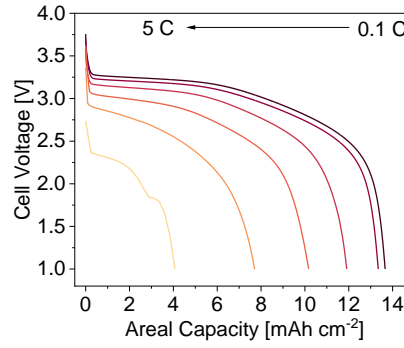
25.4 mg cm^{-2}



60.7 mg cm^{-2}



136.9 mg cm^{-2}



296 mg cm^{-2}

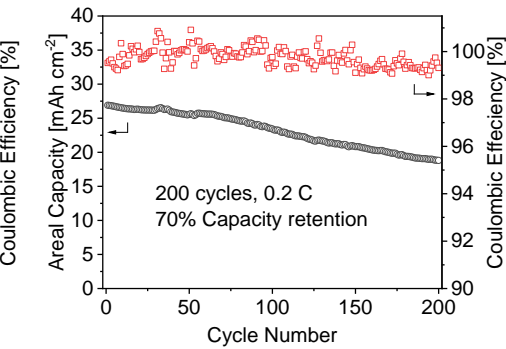
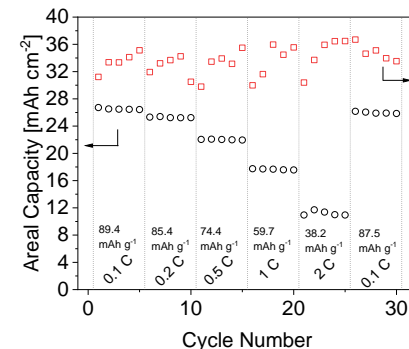
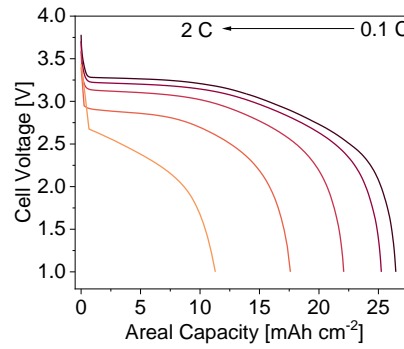


Figure S31 Detailed electrochemical data of full cells made of co-ESP NVPC/CNTF cathodes and HC/CNTF anodes of different areal loading

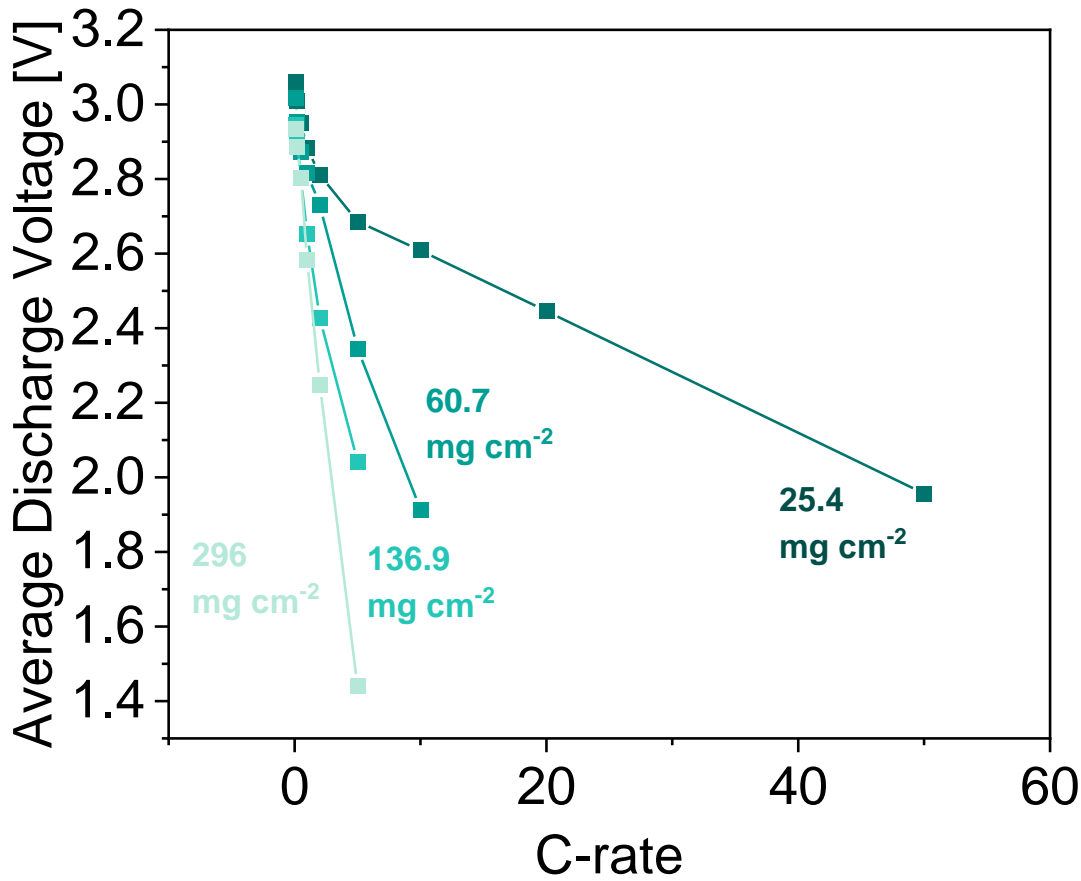


Figure S32 Average discharge voltage of co-ESP full-cells of different areal loading and C-rate

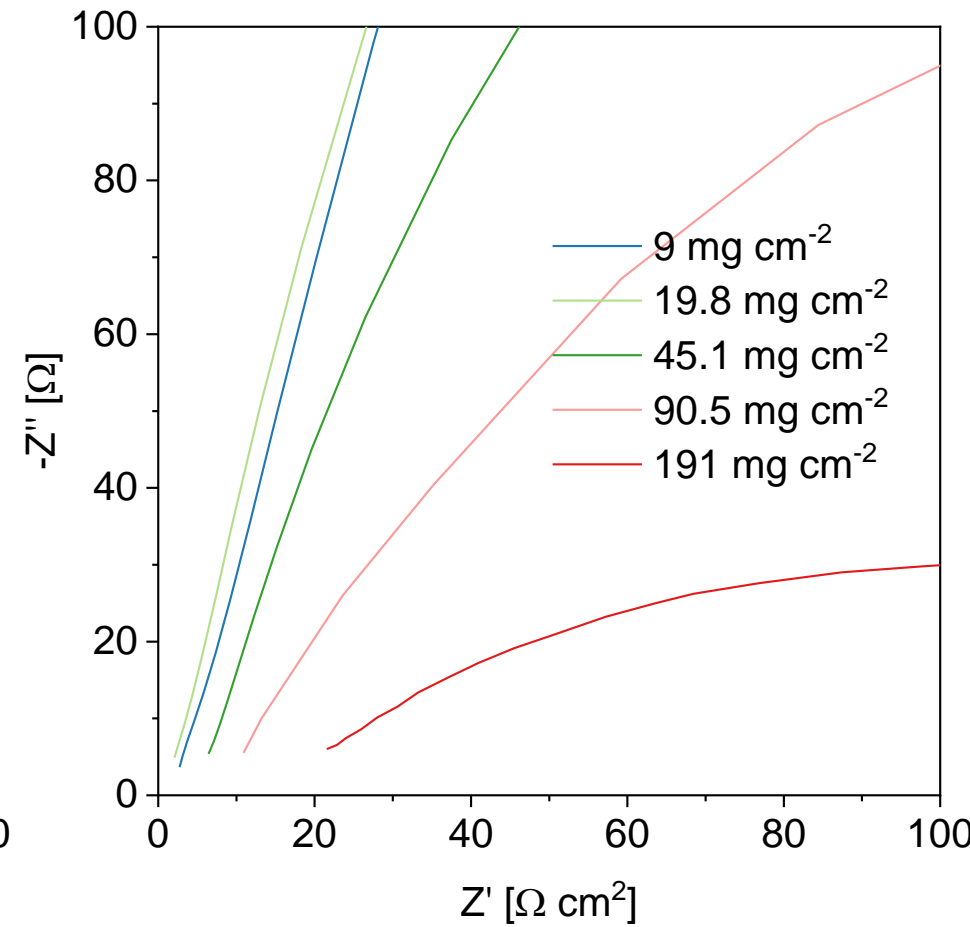
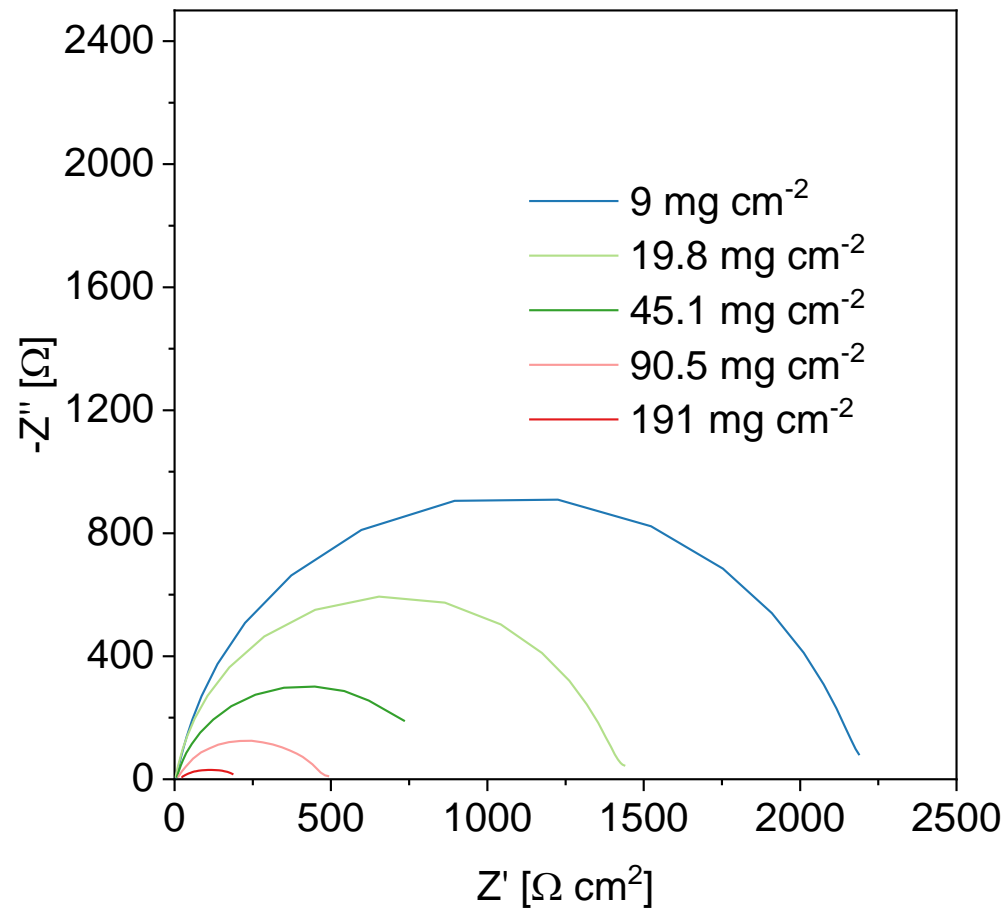


Figure S33 EIS of full cells made of co-ESP NVPC/CNTF cathodes and HC/CNTF anodes, of different cathode loading

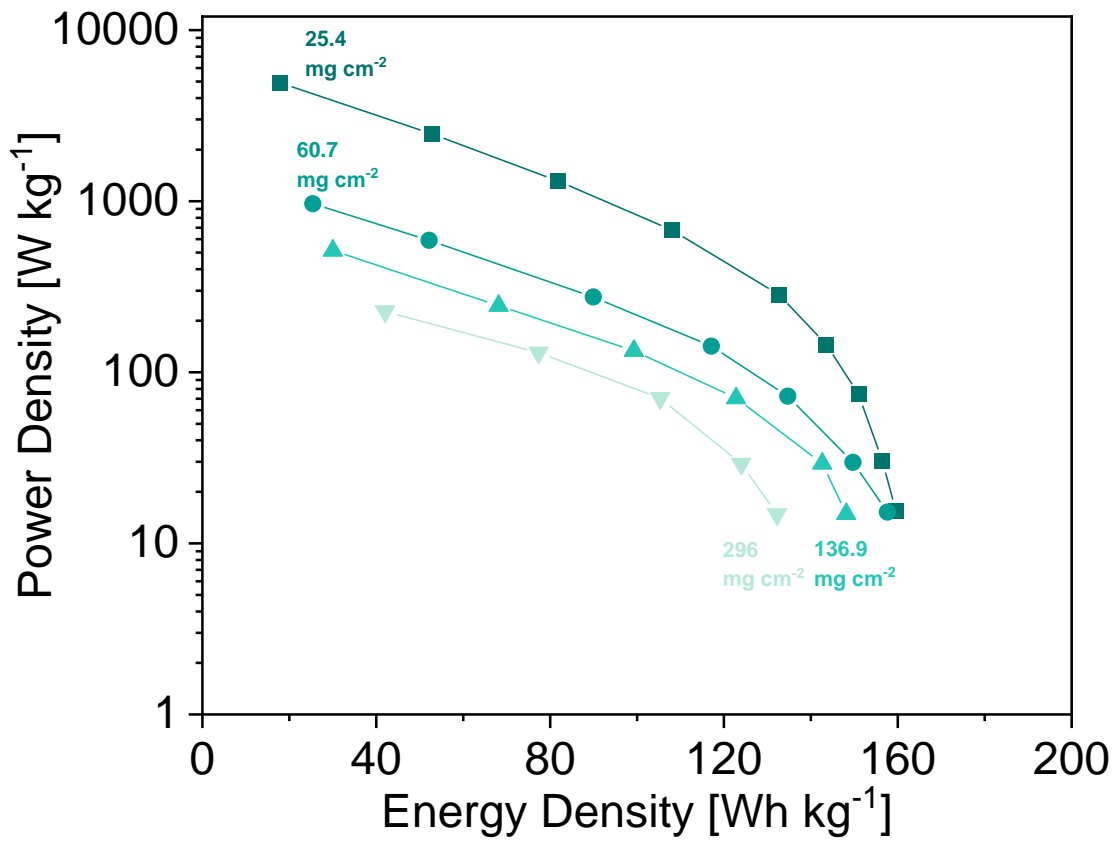


Figure S34 Gravimetric energy/power density of co-ESP full cells considering weight of electrolyte and separator

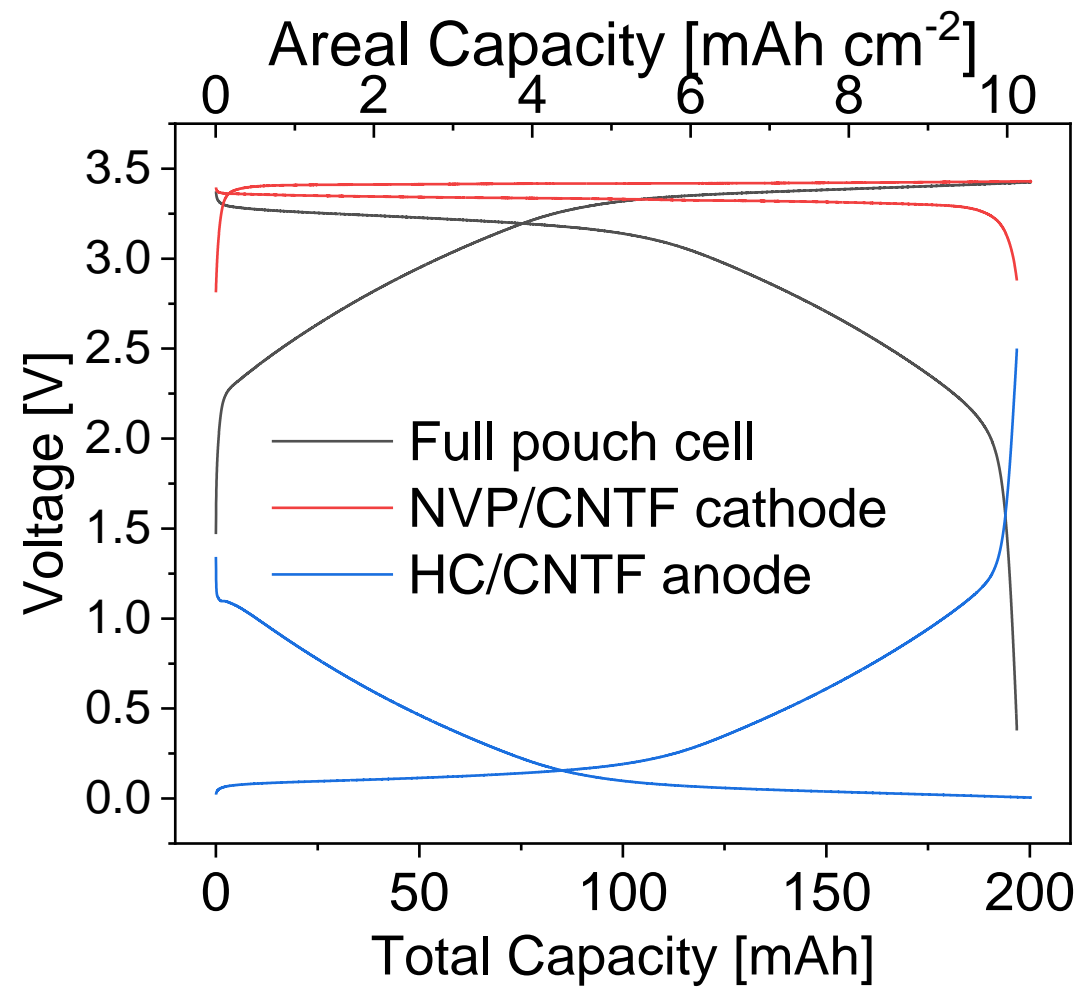


Figure S35 Voltage profiles of a single-layer, 200 mAh pouch cell with 100 mg cm⁻² areal loading, 0.2 C, with a three-electrodes set-up. CC-CV cycles. The discharge stopped when the anode's voltage reach 2.5V, or the cathode's voltage reach 2.5V, whichever happened first.

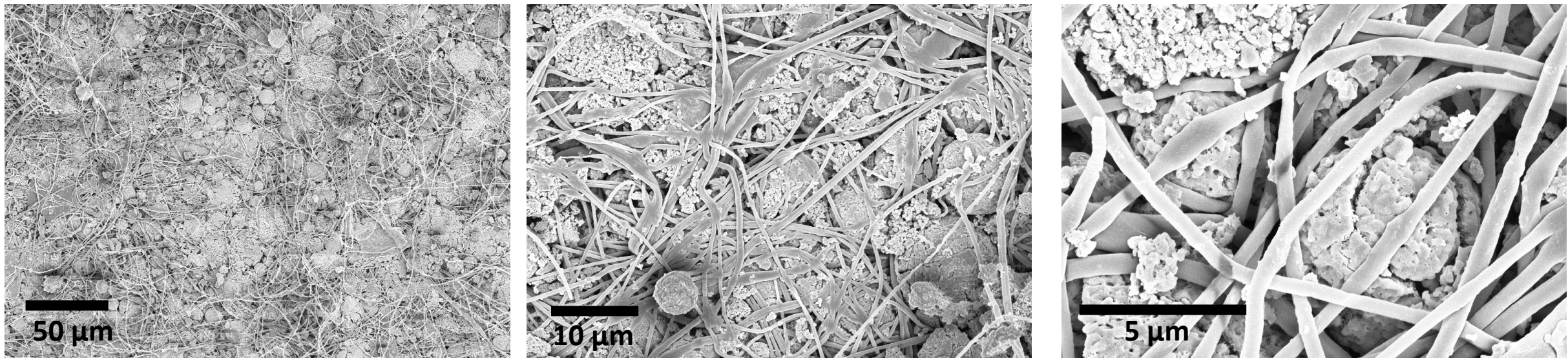


Figure S36 SEM images of the co-ESP NVPC electrode in pouch cells after compressed under 30 MPa.

Supplementary Appendix 2: Tables

Table S1 Weight of different components for electrospinning and electrospraying, for electrodes with different active content, per 1000 mg NVP cathode

Active content	Electrospraying recipe			Electrospinning recipe		
	NVPC/mg	PEO/mg	DMF/mL	PAN/mg	CNT/mg	DMF/mL
90 wt%	10 ³	200	1	200	40	4
95 wt%	10 ³	200	1	100	20	2
97.5 wt%	10 ³	200	1	50	10	1
98 wt%	10 ³	200	1	40	8	0.8
99 wt%	10 ³	200	1	20	4	0.4

Table S2 Microstructural parameters extracted from micron and nano-XCT

	Synchrotron Micro-XCT uncompressed ¹	Synchrotron Micro- XCT compressed	Nano-XCT uncompressed	Calculated compressed electrode parameters ²
Total Porosity [vol%]	90	49.3	93.1	55.8
Porosity inside particles [vol%]	N/A	N/A	4.2	28.7
Porosity outside particles [vol%]	90	49.3	88.9	27.1
NVPC volume fraction [vol%]	10	50.7	6.5	41.6
CNTF volume fraction [vol%]	N/A	N/A	0.4	2.6
Pore through-plane tortuosity	1.15	2.00	1.33	2.00
Pore in-plane tortuosity (average x/y direction)	1.09	1.68	1.12	1.68

1. The voxel size of micron-CT was 350 nm, nano-CT 47 nm

2. Because of the large field of view of micro-CT, the following parameters were acquired from micro-CT results: porosity outside particles, NVPC volume fraction, through-plane and in-plane tortuosities. Micro-CT was unable to resolve the CNTF fibres and the intra-particle pores. Therefore, the CNTF volume fraction, porosity inside particles were acquired from nano-CT results.

Table S3 co-ESP composition 97.5 wt% NVP/CNF fabric electrode on a 300 cm² substrate

Aimed areal loading [mg cm ⁻²]	Electrospraying recipe			Electrospinning recipe		
	NVP/mg	PEO/mg	DMF/mL	PAN/mg	CNT/mg	DMF/mL
5	1.5×10 ³	30	1.5	75	15	1.5
20	6×10 ³	120	6	300	60	6
100	3×10 ⁴	600	30	1.5×10 ³	300	30

Table S4 Performance comparison with published sodium-ion half batteries work

Electrode fabrication method	Cathode composition ¹	Max half cell areal loading/capacity ³ (areal loading: rate, areal capacity) ²	Rate Capacity and retention (discharge rate, specific capacity in mAh g ⁻¹ , capacity retention) ³	Half cell cycling (number of cycles, rate, capacity retention)	Max areal Energy Density (mWh cm ⁻²)/Power Density (mW cm ⁻²) ⁴	Max gravimetric energy density (Wh kg ⁻¹)/power density (W kg ⁻¹) ⁴	Ref
Co-ESP	97.5% Commercial NVPC/CNTF	49.6 mg cm ⁻² : 0.1C, 5.2 mAh cm ⁻² ; 10C, 1.9 mAh cm ⁻²	0.1C, 106.7, 91.2%; 10C, 49.1, 42%	200 cycles, 0.2C, 93.1%	20.5/145.4	336.4/2390.7	This work
		4.3 mg cm ⁻² : 0.1C, 0.48 mAh cm ⁻² ; 200C, 0.18 mAh cm ⁻²	0.1C, 111.6, 95.4%; 200C, 41.9, 35.8%	5000 cycles, 50C, 84.8%	1.59/183.4	362.2/41805	
Slurry-casting	79.5% HNVP/CB/PVDF/Al foil	48.9 mg cm ⁻² : 0.01C, 3.8 mAh cm ⁻² ; 0.5C, 1.1 mAh cm ⁻²	0.05C, 77, 70.1%; 0.5C, 23, 20.9%	48.9 mg cm ⁻² no cycling data	13.1/7.52	213.1/122.3	Ref 61
Phase inversion	76% NVP/carbon	30 mg cm ⁻² : 0.1C, 2.8 mAh cm ⁻² ; 2C, 1.4 mAh cm ⁻²	0.1C, 91.7, 78.4%; 2C, 46, 39.3%	30 mg cm ⁻² no cycling data	9.15/8.46	231.7/440.8	Ref 7
Spray-drying#	66.2% NVP/CB/PVDF/Al foil	10 mg cm ⁻² : 0.2C, 1.2 mAh cm ⁻² ; 10C, 0.27 mAh cm ⁻²	0.2C, 120, 102.5%; 10C, 29, 24.8%	100 cycles, 1C, 100%	4.02/3.2	266.1/1725.8	Ref 4
Slurry-casting	57.6% NVP@C@CNT/CB/PVDF/Al foil	10 mg cm ⁻² : 0.5C, 1.2 mAh cm ⁻² ; 30C, 0.36 mAh cm ⁻²	0.5C, 117, 100%; 30C, 36, 30.8%	450 cycles, 15C, 95.2%	3.98/80.4	229.1/4631	Ref 5
Hydrothermal	43% NCO/Ni foam	10 mg cm ⁻² : 0.33C, 1.66 mAh cm ⁻² ; 2.1C, 1 mAh cm ⁻² ,	0.33C, 166.3, 98.5%; 2.1C, 100.5, 60.4%	100 cycles, 1C, 100%	4.42/5.67	190.2/243.8	Ref 6
Sol-gel	51.9% NVP/CNF/C65/PVDF/Al foil	8.5 mg cm ⁻² : 0.1C, 0.89 mAh cm ⁻² ; 2C, 0.84 mAh cm ⁻²	0.1C, 105, 89.7%; 2C, 99.6, 85.1%	200 cycles, 2C, 100%	3.01/81.6	184.5/4992	Ref 66
Slurry-casting	56% NVPF/GO/CB/PVDF/Al foil	8 mg cm ⁻² : 0.4C, 0.98 mAh cm ⁻² ; 6.3C, 0.85 mAh cm ⁻²	0.4C, 123, 96.9%; 6.3C, 106, 83%	200 cycles, 3 C, 96%	3.64/21.8	254.8/1523.2	Ref 67
Slurry-casting	49.6% NVP/CNF/C	8 mg cm ⁻² : 0.1C, 0.82 mAh cm ⁻² ; 40C, 0.5 mAh cm ⁻²	0.1C, 103, 88%; 40C, 62, 53%	500 cycles, 1C, 95.9%	2.76/83.2	171.1/5158.4	Ref 68
Precipitation&	72.6% NVP/CNF/C	7.6 mg cm ⁻² : 0.05C, 0.87 mAh cm ⁻² ; 100C, 0.5 mAh cm ⁻²	0.05C, 114, 97.4%; 100C, 66, 56.4%	700 cycles, 1C, 89.7%	2.85/ NA	270/ NA	Ref 69

The reported capacity exceeded the theoretical value of the cathode material, the source did not specify the reason.

& The work did not give the voltage profile at higher C-rate.

1. Calculated from the highest areal loading reported in the publication that has rate and cycling data. Estimated 15 µm-thick aluminium current collector weight: 4 mg cm⁻², 10 µm-thick copper current collector: 9 mg cm⁻²

2. Showing the areal capacity from the lowest and highest cycling rate.

3. The specific capacity of the highest areal loading reported in the publication, capacity retention at different rate; NMC811's theoretical capacity is 200 mAh g⁻¹; LCO's theoretical capacity is 170 mAh g⁻¹.

4. The energy/power densities are re-calculated considering the weight and volume of all electrode components, including active material, current collector, binder, conductive additive, based on the data reported in the literature. The method of calculation is shown in Supplementary Appendix 4.

Table S5 Performance comparison with published lithium-ion half-cell work

Fabrication method	Cathode composition ¹	Max half cell areal loading/capacity ³ (areal loading: rate, areal capacity) ²	Rate Capacity and retention (discharge rate, specific capacity in mAh g ⁻¹ , capacity retention) ³	Half cell cycling (number of cycles, rate, capacity retention)	Max areal Energy Density (mWh cm ⁻²)/Power Density (mW cm ⁻²) ⁴	Max gravimetric energy density (Wh kg ⁻¹)/power density (W kg ⁻¹) ⁴	Ref
Co-ESP	97.5% Commercial NVPC/CNTF	49.6 mg cm ⁻² : 0.1C, 5.2 mAh cm ⁻² ; 10C, 1.9 mAh cm ⁻²	0.1C, 106.7, 91.2%; 10C, 49.1, 42%	200 cycles, 0.2C, 93.1%	20.5/145.4	336.4/2390.7	This work
		4.3 mg cm ⁻² : 0.1C, 0.48 mAh cm ⁻² ; 200C, 0.18 mAh cm ⁻²	0.1C, 111.6, 95.4%; 200C, 41.9, 35.8%	5000 cycles, 50C, 84.8%	1.59/183.4	362.2/41805	
Mechanical pressing	79% LCO/KB/Carbon Cloth	71 mg cm ⁻² : 0.08C, 10 mAh cm ⁻² ; 0.8C, 8.7 mAh cm ⁻²	0.08C, 137, 85.6%; 1.6C, 97, 60.6%	40 cycles, 0.15C, 91%	37.7/50.4	419.9/709.9	ref
Slurry-casting&	80% LCO/cellulose/CNT	86 mg cm ⁻² : 0.1C, 12.1 mAh cm ⁻²	0.1 C, 141, 88.1%; no rate	20 cycles, 0.04C, 90%	46/5.23	427.7/48.6	ref
Impregnation	100% LCO	206 mg cm ⁻² : 0.05C, 24.7 mAh cm ⁻² ; 1C, 7.79 mAh cm ⁻²	0.05 C, 120, 75%; 1C, 37.8, 23.6%	27 cycles, 0.5C, 87%	93.9/95.6	455.6/464	ref
Slurry-casting	90.2% NMC811/biopolymer/CNT/Al foil	47.7 mg cm ⁻² : 0.1C, 8.84 mAh cm ⁻² ; 1C, 3 mAh cm ⁻²	0.05C, 185, 92.5%; 1C, 62.9, 31.4%	50 cycles, 0.2C, 92.5%	29.9/28.9	625.8/604.3	ref
Slurry-casting	75% LFP/kb/CNF/PVDF	108 mg cm ⁻² : 0.05C, 17 mAh cm ⁻² ; 0.5C, 10 mAh cm ⁻²	0.05C, 157.4, 92.6%; 0.5C, 92.6. 54.5%	40 cycles, 0.2C, 94.3%	57.5/26.8	399/190	ref
Slurry-casting	71% LFP/CB/PVDF/Al foil	128 mg cm ⁻² : 0.025C, 19.8 mAh cm ⁻² ; 1C, 0.81 mAh cm ⁻²	0.025C, 155, 91.2%; 1C, 6.34, 3.7%	150 cycles, 0.1C, 73%	65.3/56	358.1/310.6	ref
Slurry-casting&	95.7% NMC811/CNT/Al foil	99 mg cm ⁻² : 0.05C, 17.8 mAh cm ⁻² ; 0.25C, 7.2 mAh cm ⁻²	0.05C, 180, 90%; 0.25C, 72.7, 36.4%	10 cycles, 0.1C, 96%	65.9/ NA	631.2/ NA	ref
Slurry-casting&	80% LFP/CNT/EVA	49 mg cm ⁻² : 0.2C, 7.5 mAh cm ⁻² ; 2C, 3 mAh cm ⁻²	0.2C, 153.1, 90%; 2C, 61.2, 36%	N/A	24.4/NA	416.3/NA	ref
Slurry-casting	67.3% LFP/CB/PVDF	70 mg cm ⁻² : 0.05C, 10.9 mAh cm ⁻² ; 1C, 1.5 mAh cm ⁻²	0.05C, 155.7, 91.6%; 1C, 21.4, 12.6%	200 cycles, 0.1C, 70%	36/16.4	346.1/157.7	ref
Extrusion	93.9 % LFP/carbon/Al foil	90 mg cm ⁻² : 1/24C, 12.8 mAh cm ⁻² ; 1/12C, 11.1 mAh cm ⁻²	1/24C, 142.2, 83.6%; 1/12C, 123.3, 72.5%	7 cycles, 1/12C, 86.6%	42.2/4.2	440.3/43.8	ref
Hot-pressing&	76.5% NMC712/CNT/PVDF/Al foil	70 mg cm ⁻² : 0.1C, 13.2 mAh cm ⁻² ; 0.5C, 6.8 mAh cm ⁻²	0.1C, 188.6, 94.3%; 0.5C, 97.1, 48.6%	30 cycles, 0.1C, 96%	48.8/NA	533.3/NA	ref

& The work did not give the voltage profile at higher C-rate.

1. Calculated from the highest areal loading reported in the publication that has rate and cycling data. Estimated 15 µm-thick aluminium current collector weight: 4 mg cm⁻², 10 µm-thick copper current collector: 9 mg cm⁻²

2. Showing the areal capacity from the lowest and highest cycling rate.

3. The specific capacity of the highest areal loading reported in the publication, capacity retention at different rate; NMC811's theoretical capacity is 200 mAh g⁻¹; LCO's theoretical capacity is 170 mAh g⁻¹.

4. The energy/power densities are re-calculated considering the weight and volume of all electrode components, including active material, current collector, binder, conductive additive, based on the data reported in the literature. The method of calculation is shown in Supplementary Appendix 4.

Table S6 Fabrication composition of co-ESP hard carbon

Aimed areal loading [mg cm ⁻²]	Electrospraying recipe			Electrospinning recipe		
	NVP/mg	PEO/mg	DMF/mL	PAN/mg	CNT/mg	DMF/mL
5	1.5×10 ³	600	3	160	32	3.2
10	3×10 ³	1.2×10 ³	6	320	64	6.4
25	7.5×10 ³	3×10 ³	15	800	160	16
40	1.2×10 ⁴	4.8×10 ³	24	1.28×10 ³	256	25.6

Table S7 Specification of sodium-ion battery coin cell using co-ESP electrodes, 25.4 mg cm⁻² cathode loading

	Separator	Cathode	Anode
Active materials used	Polypropylene	NVPC/CNTF	Hard carbon/CNTF
Active materials loading [wt%]	N/A	97.5 %	98 %
Conductive additive [wt%]		2.5%	2 %
Binder [wt%]			
Current collector [wt%]			
Areal loading [mg cm⁻²]		25.4	3.9
Compressed thickness [μm]	25	136.1	92.1
Area [cm²]	2.3	0.78	1.77
Total Weight [mg]	3	20.3	7
Electrolyte weight [mg]¹	11.6		
Energy density gravimetric [Wh kg⁻¹]²	156.4	Cell areal capacity 0.2 C [mAh cm⁻²]	2.63

1. The electrolyte weight is calculated by: $W_{electrolyte} = V_{cell}\varphi\rho_{electrolyte}$, $V_{electrode}$ is the volume of the electrodes and separator, φ is the porosity of the electrodes and separator, $\rho_{electrolyte}$ is the density of the electrolyte.
2. Including the weight of electrode components, separator, and electrolyte

Table S8 Specification of sodium-ion battery coin cell using co-ESP electrodes, 296 mg cm⁻² cathode loading

	Separator	Cathode	Anode
Active materials used	Polypropylene	NVPC/CNTF	Hard carbon/CNTF
Active materials loading [wt%]	N/A	97.5 %	98 %
Conductive additive [wt%]		2.5%	2 %
Binder [wt%]			
Current collector [wt%]			
Areal loading [mg cm⁻²]		296	46
Compressed thickness [μm]	25	1586	1086
Area [cm²]	2.3	0.78	1.77
Total Weight [mg]	3	236.8	83
Electrolyte weight [mg]¹	135		
Energy density gravimetric [Wh kg⁻¹]²	124	Cell areal capacity 0.2 C [mAh cm⁻²]	26.4

1. The electrolyte weight is calculated by: $W_{electrolyte} = V_{cell}\varphi\rho_{electrolyte}$, $V_{electrode}$ is the volume of the electrodes and separator, φ is the porosity of the electrodes and separator, $\rho_{electrolyte}$ is the density of the electrolyte.
2. Including the weight of electrode components, separator, and electrolyte

Table S9 Specification of sodium-ion battery coin cell using conventional electrodes

	Separator	Cathode	Anode
Active materials used	Polypropylene	NVPC	Hard carbon
Active materials loading [wt%]	N/A	69.8 %	29.3 %
Conductive additive [wt%]		3.1 %	0 %
Binder [wt%]		4.6 %	3.3 %
Current collector [wt%]¹		22.5 %	67.4 %
Areal loading [mg cm⁻²]		16	3.9
Thickness [μm]	25	110	62
Area [cm²]	2.3	1.1	1.9
Weight [mg]	3	25.2	25.3
Electrolyte weight [mg]²	10.1		
Energy density gravimetric [Wh kg⁻¹]³	89.5	Cell areal capacity 0.2 C [mAh cm⁻²]	1.7

1. Estimated 15 μm-thick aluminium current collector weight: 4 mg cm⁻², 10 μm-thick copper current collector: 9 mg cm⁻².
2. The electrolyte weight is calculated by: $W_{electrolyte} = V_{cell}\varphi\rho_{electrolyte}$, $V_{electrode}$ is the volume of the electrodes and separator, φ is the porosity of the electrodes and separator, $\rho_{electrolyte}$ is the density of the electrolyte, 1.26 g mL⁻¹.
3. Including the weight of electrode components, separator, and electrolyte

Table S10 Performance comparison with published sodium-ion full batteries work

Fabrication method	Cathode composition ¹	Max cathode areal loading/capacity (areal loading: rate, areal capacity) ²	Rate Capacity and retention (discharge rate, specific capacity in mAh g ⁻¹ , capacity retention) ³	Anode composition ¹	Full cell cycling (number of cycles, rate, capacity retention)	Max areal Energy Density (Wh cm ⁻²)/Power Density (W cm ⁻²) ⁴	Max gravimetric Energy Density (Wh kg ⁻¹)/Power Density (W kg ⁻¹) ⁴	Ref
Co-ESP	97.5% Commercial NVP/CNT/CNF, no binder, no current collector	296 mg cm ⁻² : 0.1C, 26.5 mAh cm ⁻² ; 1C, 11 mAh cm ⁻²	0.1C, 89.4, 76.4%; 2C, 46.5, 39.7%	98% Hard carbon-CNF/CNT, no binder, no current collector	200 cycles, 0.2C, 84.7%	77.7/133.1	191.9/328.8	This work
		25.4 mg cm ⁻² : 0.1C, 2.64 mAh cm ⁻² ; 50C, 0.47 mAh cm ⁻²	0.1C, 103.8, 88.7%; 50C, 42.7, 36.5%		200 cycles, 0.2C, 96.2%	8.05/248.4	231.6/7152.6	
Phase inversion	76% NVP/carbon, no binder, no current collector	7 mg cm ⁻² : 0.1C, 0.7 mAh cm ⁻² ; 2C, 0.6 mAh cm ⁻²	0.1C, 102, 87.2%; 2C, 89, 76.1%	Hard carbon, composition unspecified	100 cycles, 1C, 99%	2.14/3.71	147.2/254.1	Ref 7
Sol-gel	51.9% NVP/CNF/C65/PVDF/Al foil	8.5 mg cm ⁻² : 0.1C, 0.85 mAh cm ⁻² ; 2C, 0.76 mAh cm ⁻²	0.1C, 99.7, 85.2%; 2C, 90, 76.9%	51.9% NVP/CNF/C65/PVDF/Al foil	3000 cycles, 2C, 60.1%	1.47/195.5	45/5968.5	Ref 66
Precipitation	72.6% NVP/CNF/C, no binder, no current collector	7.6 mg cm ⁻² : 0.05C, 0.84 mAh cm ⁻² ; 100C, 0.41 mAh cm ⁻²	0.05C, 111, 94.7%; 100C, 54.5, 46.6%	76.5% NTP/CNF/C, no binder, current collector	1000 cycles, 1C, 91% 4000 cycles, 20C, 74.5%	1/72.2	49.3/3538.7	Ref 69
Slurry-casting	56% NVPF/GO/CB/PVDF/Al foil	8 mg cm ⁻² : 0.78C, 0.88 mAh cm ⁻² ; 6.3C, 0.74 mAh cm ⁻²	0.78C, 110, 85.9%; 6.3C, 92.5, 72.3%	18.7% SnP/GO/CB/PA/Al foil	200 cycles, 0.78C, 62%	2.13/18.4	109.5/1840	Ref 67
Slurry-casting	25.6% NVP@C@CNT/CB/PVD F/Al foil	1.5 mg cm ⁻² : 0.05C, 0.77 mAh cm ⁻² ; 25C, 0.45 mAh cm ⁻²	0.05C, 102, 87.2%; 25C, 60, 51.2%	25.7% mesocarbon/CB/CMC-SBR/Al foil	5000 cycles, 5C, 72.7%	0.37/74.2	31.3/6366	Ref 5
Slurry-casting	31.5% HNVP/CB/PVDF/Al foil	2 mg cm ⁻² : 0.5C, 0.18 mAh cm ⁻² ; 20C, 0.12 mAh cm ⁻²	0.5C, 90.8, 82.7%; 20C, 61.8, 56.3%	31.5% NTP/CB/PVDF/Alfoil	700 cycles, 2C, 88.8%	0.23/5.27	17.9/414.9	Ref 61

1. Calculated from the highest areal loading reported in the publication that has rate and cycling data. Estimated 15 µm-thick aluminium current collector weight: 4 mg cm⁻², 10 µm-thick copper current collector: 9 mg cm⁻²

2. Showing the areal capacity from the lowest and highest cycling rate.

3. The specific capacity of the highest areal loading reported in the publication, capacity retention at different rate; NMC811's theoretical capacity is 200 mAh g⁻¹; LCO's theoretical capacity is 170 mAh g⁻¹.

4. The energy/power densities are re-calculated considering the weight and volume of all electrode components, including active material, current collector, binder, conductive additive, based on the data reported in the literature. The method of calculation is shown in Supplementary Appendix 4.

Table S11 Performance comparison with published lithium-ion full batteries work

Fabrication method	Cathode composition ¹	Max cathode areal loading/capacity (areal loading: rate, areal capacity) ²	Rate Capacity and retention (discharge rate, specific capacity in mAh g ⁻¹ , capacity retention) ³	Anode composition ¹	Full cell cycling (number of cycles, rate, capacity retention)	Max areal Energy Density (Wh cm ⁻²)/Power Density (W cm ⁻²) ⁴	Max gravimetric Energy Density (Wh kg ⁻¹)/Power Density (W kg ⁻¹) ⁴	Ref
Co-ESP	97.5% Commercial NVPC/CNTF, no binder, no current collector	296 mg cm ⁻² : 0.1C, 26.5 mAh cm ⁻² ; 11 mAh cm ⁻² , 2C	0.1C, 89.4, 76.4%; 2C, 46.5, 39.7%	98% Hard carbon/CNTF, no binder, no current collector	200 cycles, 0.2C, 84.7%	77.7/133.1	191.9/328.8	This work
		25.4 mg cm ⁻² : 0.1C, 2.64 mAh cm ⁻² ; 50C, 0.47 mAh cm ⁻²	0.1C, 103.8, 88.7%; 50C, 42.7, 36.5%		200 cycles, 0.2C, 96.2%	8.05/248.4	231.6/7152.6	
Slurry-casting	80% LCO/cellulose/CNT, no current collector	30 mg cm ⁻² : 0.1C, 4.6 mAh cm ⁻² ; 1C, 2.8 mAh cm ⁻²	0.1C, 152, 89.4%; 1C, 93.3, 54.9%	80% LTO/cellulose/CNT	N/A	10.6/10.5	141.3/140	ref
Slurry-casting	94.5% NMC811/biopolymer/CNT/Al foil	54.4 mg cm ⁻² : 0.1C, 9.24 mAh cm ⁻² No rate data	0.1C, 169.9, 85% No rate data	Graphite/biopolymer/CNT/Cu foil, unknown active content, max 76.9%	40 cycles, 0.1C, 92.8%	33.3/3.6	367.9/66.2	ref
Slurry-casting	96.4% NMC811/CNT/Al foil	156 mg cm ⁻² : 1/15C, 29 mAh cm ⁻² ; 1C, 15 mAh cm ⁻²	0.05C, 185.9, 93%; 1C, 96.2, 48.1%	52.1% Si/CNT/Cu foil	47 cycles, 1/15C, 83%	98.3/105.8	569.3/586.6	ref
Impregnation	62.2% LFP/Super P/PVDF/CNT-polyester current collector	168 mg cm ⁻² : 1/15C, 26 mAh cm ⁻² ; No rate data	1/15C, 155, 91.2% No rate data	61.1% LTO/Super P/PVDF/CNT-polyester current collector	33 cycles, 0.1C, 86%	46.8/3.4	85.7/6.2	ref
Extrusion	93.9 % LFP/carbon/Al foil	90 mg cm ⁻² : 1/24C, 150, 88.2%; 1/12C, 123, 72.4%	1/24C, 150, 88.2%; 1/12C, 123, 72.4%	92.2% LTO/carbon/Cu foil	100 cycles, 1/12C, 67%	23.6/14.2	121.9/73.3	ref
Slurry-casting	80% LFP/carbon/EVA, no current collector	29.4 mg cm ⁻² : 0.1C, 4.6 mAh cm ⁻² ; 1C, 3.5 mAh cm ⁻²	0.1C, 156.5, 92%; 1C, 120, 70.5%	80% LTO/carbon/EVA	60 cycles, 0.5C, 76.9%	8/8.5	108.8/115.6	ref
Slurry-casting	65% LFP/CB/PVDF, no current collector	36 mg cm ⁻² : 0.05C, 5.5 mAh cm ⁻² ; 0.1C, 5 mAh cm ⁻²	0.05C, 152.8, 89.9%; 0.1C, 138.9, 81.7%	59% LTO/CB/PVDF	500 cycles, 0.1C, 87%	9.9/1.1	85.3/9.5	ref

1. Calculated from the highest areal loading reported in the publication that has rate and cycling data. Estimated 15 µm-thick aluminium current collector weight: 4 mg cm⁻², 10 µm-thick copper current collector: 9 mg cm⁻²

2. Showing the areal capacity from the lowest and highest cycling rate.

3. The specific capacity of the highest areal loading reported in the publication, capacity retention at different rate; NMC811's theoretical capacity is 200 mAh g⁻¹; LCO's theoretical capacity is 170 mAh g⁻¹.

4. The energy/power densities are re-calculated considering the weight and volume of all electrode components, including active material, current collector, binder, conductive additive, based on the data reported in the literature. The method of calculation is shown in Supplementary Appendix 4.

Table S12 An indicative raw material cost estimation of co-ESP method and conventional method

Co-ESP method	NVPC/kg	PEO/kg	PAN/kg	CNT/kg	DMF/mL	Full electrode
Amount (kg)	0.975	0.0195	0.04875	0.00975	1.95	
\$ per kg		10	5	35	0.66	
Cost (\$)		0.195	0.24375	0.34125	1.287	2.067
Conventional method	NVPC/kg	PVDF/kg	Carbon black/kg	Al foil/kg	NMP/mL	Full electrode
Amount (kg)	0.95	0.02	0.03	0.16	1.67	
\$ per kg		14	10	35	1.4	
Cost (\$)		0.28	0.3	5.6	2.338	8.518

This table present the breakdown raw materials' cost for producing 1 kg of NVPC electrodes at a loading of 25 mg cm^{-2} (excluding current collector), using both the co-ESP and conventional methods. The composition of co-ESP is based on the 97.5 wt. % loading co-ESP NVPC electrode used in this work. The composition of slurry-casted electrode is based on the conventional electrode presented in **Figure 2j**. The solid loading of the electrode slurry is standard 60 wt.%. The raw materials cost are obtained from www.echemi.com and from suppliers at www.alibaba.com.

Supplementary Appendix 3: Calculating Energy Density

- The gravimetric energy densities were calculated by: $E_g = \bar{V} C_g c_{active}$. \bar{V} is the average voltage in the discharge process; C_g is the gravimetric specific capacity, considering only the weight of active materials; c_{active} is the active content, calculated by :
- $c_{active} = \frac{m_{active}}{m_{active} + m_{binder} + m_{current\ collector} + m_{conductive\ additive}}$. Estimated 15 μm -thick aluminium current collector weight: 4 mg cm^{-2} , 10 μm -thick copper current collector: 9 mg cm^{-2}
- The gravimetric power densities were calculated by: $P_g = I_g \bar{V} c_{active}$. I_g is the discharge gravimetric current density, calculated by : $I_g = \frac{I}{m_{active}}$. I is the discharge current.
- The areal energy densities were calculated by: $E_a = \bar{V} C_a$. C_a is the areal capacity.
- The areal power densities were calculated by: $E_a = \bar{V} I_a$. I_a is the areal current, calculated by $I_a = \frac{I}{A_{electrode}}$, $A_{electrode}$ is the geometric area of the electrode.
- The energy densities in all referenced literatures in **Figure 4h, i, Figure 5e, f, Table S4, S5, S10, S11** were recalculated with the above formula, to make consistent comparisons.
- To calculate the gravimetric energy/power density considering the electrolyte and separator in **Figure S34**, we substitute the c_{active} in the equation with $c'_{active} = \frac{m_{active}}{m_{active} + m_{binder} + m_{current\ collector} + m_{conductive\ additive} + m_{electrolyte} + m_{separator}}$. $m_{separator}$ is 3.1 mg for a 2.5 cm^2 Celgard 2400 separator. $m_{electrolyte} = \rho_{electrolyte} v_{composite} P$, P is the porosity of the electrodes/separator composite, $v_{composite}$ is the volume of the composite, $\rho_{electrolyte}$ is the electrolyte's density, 1.26 g cm^{-3} .
- To calculate the gravimetric energy density of pouch cells, the $c'_{active}^{pouch} = \frac{m_{active}}{m_{pouch}}$. The volumetric energy density of the pouch cells were calculated by: $E_g = \frac{\bar{V} C}{A_{pouch} L_{pouch}}$. A_{pouch} is the geometric area of the pouch cell, L_{pouch} is the thickness.